PRELIMINARY COPY

ELECTROCHEMISTRY OF SILVER-SILVER CHLORIDE ELECTRODES

by

T. L. Johnson
W. Kohn
B. Salzsieder
J. E. Wall

Abstract

This memorandum describes laboratory measurements and theoretical research carried out under the first phase of NSF Grant 75-02562, "Electrodes and the Measurement of Bioelectric Phenomena". The experimental work clearly demonstrates the need for improved models. A complete but still preliminary model based on nonequilibrium thermodynamics is presented. The results of a literature search are also summarized.

Electronic Systems Laboratory
Department of Electrical Engineering and Computer Science
Massachusetts Institute of Technology
Cambridge, Massachusetts 02139

Table of Contents

Preface

Our long-range goal is the design of filters for the estimation of bioelectric source events based on electrode measurements. The remarkable success of optimal filtering techniques for finite-dimensional systems is based largely on their effective use of a model for the dynamics of the system generating and/or distorting the available measurements.

Boundary measurements on a distributed system such as the human body exhibit dynamic characteristics which cannot be adequately represented as properties of outputs of finite-dimensional time-invariant (possibly linear) systems. The appearance of time-delay, hysteresis-like effects, and nonrational spectra are a few examples. In order to design adequate filters for such signals using any type of "internal model principle"--we thus require a thorough distributed model of the measurement process. Simplification or approximation of such a model, of course, would generally be necessary for filter design.

The objective of the initial stage of this research is to develop a model based on physical principles which exhibits dynamical properties measured in the laboratory. This document reports on the initial phases of the modelling effort and on initial laboratory experiments. It is intended as a working document rather than as a report of final results.[1] In the next phase of this research, we will identify parameters (reaction rate constants, diffusion coefficients, mole fractions, etc.) of the model, and suggest viable

---

[1] We have just recently, in fact, discovered an elegant way of treating boundary conditions which will probably supercede the boundary-layer method proposed herein.

simplifications of it. We will also progress to refined experimental techniques (in order to acquire more accurate estimates of specific parameters), and to the use of electrodes as sensors for known source signals.

The casual reader is advised to preview the concluding pages of each section to assess the nature of our results.

Physical Properties of Silver-Silver Chloride Electrodes

T. L. Johnson, W. Kohn, B. Saltzieder, and J. Wall

I.   Introduction

II.   Experimental apparatus, measurement circuits, and equipment used.

III. Summary of Experiments

    A. Plating Experiments

    B. Preliminary DC V-I Relation of Plated Electrodes

    C. Measurement of Cell Impedance with Bridge

    D. DC V-I Relation in Distilled Water

    E. Current Oscillation with Constant Voltage

    F. High-Voltage DC V-I Relation (Plated Electrode)

    G. Effect of Pressure on Open Circuit Cell Voltage

    H. Low-Voltage D.C. V-I Relation. (Bare electrode)

    I. High-Voltage D.C. V-I Relation ("   "   )

    J. Low-Voltage Transient Behavior of Bare Electrodes

    K. V-I Relation of Plated Electrodes (.01 N)

    L. V-I Relation of   "   "   (.1 N)

    M. A C Impedance Measurements

        M_1: No plating, .01 N solution

        M_2: No plating, .1 N solution

        M_3: Plated, .01 N solution

        M_4: Plated, .1 N solution

    N. Effect of Voltage on AC Impedance

IV   Discussion, Conclusions

I. Introduction

This memorandum describes a set of laboratory experiments performed during the summer of 1975 in conjunction with NSF Grant 75-02562 "Electrodes and the Measurement of Bioelectric Phenomena". The general motivation and basic equipment for these experiments is described in the Proposal document (as amended) for this research. The objectives of these experiments were to

- establish basic experimental techniques
- verify linear equivalent-circuit models of electrodes obtained by others, for sinusoidal stimuli, using our experimental apparatus
- discover salient dynamical properties, particularly nonlinearities, of the bare silver and silver-silver chloride electrodes
- define the possible chemical reactions occurring at the electrode interface
- provide order-of-magnitude parameter estimates for use in a mathematical model for electrode dynamics, as discussed in the accompanying memorandum.

Though considerable care was taken in making these measurements, the numerical data obtained are intended primarily for qualitative evaluation and are not made under sufficiently controlled conditions to be used for very through quantitative studies. In the next stage of experimentation, aimed at model verification and parameter identification, refined techniques will be used, and original experimental procedures will be devised. Thus, high accuracy, repeatable readings will be obtained.

The qualitative conclusions of these experiments are assembled in the final remarks; we first describe the various experiments.

II. **Equipment**

    A. Electrodes, Preparations

    B. Measuring Equipment

    C. Test Circuits

A. Electrodes

A.1 Test rig.

All experiments described herein are for the same test rig geometry. A large glass tube (inner diameter 2 5/16", outer diameter 2 1/2"), cut to a length of about 8" was modified by a glassblower at its midpoint by the insertion of two tubular openings (inner diameter, ~1/2") for filling and draining. A glass burette valve was attached to the drain tube. Large rubber washers (inner diameter, 2") were placed over the ends of the large cylinder, and discs cut from heavy pure silver foil* (thickness, .25mm) were placed over the ends. Glass discs were mounted behind the silver, and the whole assembly was clamped together by 3 long bolts passing through holes in the glass. No adhesives were used. No leakage of solution occurred at the edges of the washers. There were no indications in any of the experiments of any contamination or chemical activity of the rubber. Silver chloride deposits always were observed to end abruptly, and without observable edge effects, at the inner edge of the washers. The volume of the closed cylinder was approximately 600 ml.

A.2 Preparation of silver

In these preliminary studies, the silver surface was polished with

---

*Alpha Products, Beverly, Mass., type M3N, Stock #00300.

a commercial silver polish[*] and then rinsed in several changes of distilled water and/or NaCl solution prior to testing or chloriding. While no adverse effects from this method of preparation were noted (e.g., nonuniformity of chloriding), future procedures will involve cleaning in an acid bath (e.g., concentrated HCl) having low impurity content, in particular Br^+.

A.3 Preparation of Solutions

High-purity NaCl[**] was dissolved in distilled water. Concentrations were composed as follows

.01 N NaCl: .904 g. NaCl/l.
.1 N NaCl: 9.04 g. NaCl/l.

B.   Measuring Equipment

Precision, calibration, and compatibility of instrumentation is a

---

[*] <u>Cando</u> Royal Polish, J. A. Wright & Co., Keene, N. H. 03431

[**] Mallinckrodt analytical reagent 7581
        NaCl crystals-meets A.C.S. specifications

Maximum limits of impurities:

Barium (Ba)...............................To pass test (Approx. 0.001%)
Bromide (Br)..............................To pass test (Approx. 0.01%)
Calcium, Magnesium, and R_2O_3 Ppt.............................. 0.005%
Chlorate and Nitrate (as NO_3).................................. 0.003%
Heavy Metals (as Pb)... 0.0005%
Insoluble Matter.. 0.005%
Iodide (I).. 0.002%
Iron (Fe)... 0.0002%
Nitrogen Compounds (as N)....................................... 0.001%
Phosphate (PO_4).. 0.0005%
Potassium (K)... 0.005%
Sulphate (SO_4)... 0.001%
pH OF A 5% SOLUTION AT 25°C..................................... 5.0-9.0

major consideration in these experiments. Most of the experiments require
some source of AC or DC potential, the testrig, a series resistor, and
independent means of measuring voltage and current. Micropolarization
measurements require low-drift, noise-free sources and measuring devices,
and particular note must be taken of the fact that under certain conditions,
the cell actually supplies current, not behaving as a simple impedance. Digital
meters can present unpredictable impedance changes and offsets to the rest
of the circuit, and hence must be used with care. A commercial R-C bridge
gave inaccurate and conflicting measurements of the "equivalent impedance"
of the cell under various conditions (see experiment C, next section).
Care must be taken in AC measurements that the (low-impedance) cell does
not load the voltage/current source. Oscilloscope probes must be tuned to
have nearly identical characteristics. Most signal sources are designed
for regulated output voltages, but for many measurements and in the theoret-
ical model, it is more natural to use regulated current sources. Circuitry
to achieve current regulation is now being designed for future experiments,
although voltage sources were used in all measurements reported below.

A detailed list of equipment employed in the experiments is shown
below. We shall henceforth refer to most instruments by their manufacturer/
description only.

| ESL Part No.	Maker	Model	Description
383-2004	Triplett	Model 675	DC Milliammeter
Cont Lab-21	Data Precision	Model 134	Digital multimeter
8687 3	General Radio	Type 1650A	Impedance Bridge
7002-5062	Hewlett-Packard	Model 200 CD	Audio Oscillator
7849/31	General Radio	Type 1432-K	Decade Registor
CL-13	Trygon	Model HR40-3B	0-40VDC Supply
275	Sorenson	Model QRB30-1	0-30VDC Supply
70429-1	Wavetek	Model 202	Voltmeter
FC-44 7	Ad-Yu (Advanced Electronics)	Type 205	Phase Detector
7849-14	Hewlett-Packard	Model 425-A	AC Micro Volt-ammeter
SM-430	Biddle		.92 Ω Slide Resistor
2289	Eico	Model 1171	Comparator (decade resistor)
762982	Eppley	Cat. No. 100	Standard Cell
Cont. Lab 3	Tektronix	Type 564	Storage Scope
CL-6	"	Type 3A1	Dual Trace Amplifier
000144	"	Type 3B3	Time Base
9247-2	"	010-128	÷ 10 Probe
11	"	010-130	÷ 10 Probe
7002-5100	Hewlett-Packard	Model 202A	Low Freq. Funct. Gen.
(RLE)	Tektronix	Type 503	Scope
(RLE)	"	Type 535A	"
(RLE)	"	Type 1L5	Spectrum Analyzer

C. Test Circuits

Three basic test circuits were used: (1) for measuring direct-current V-I relations, (2) for measuring AC impedances, and (3) for plating. The equipment used in these circuits is noted for each experiment.
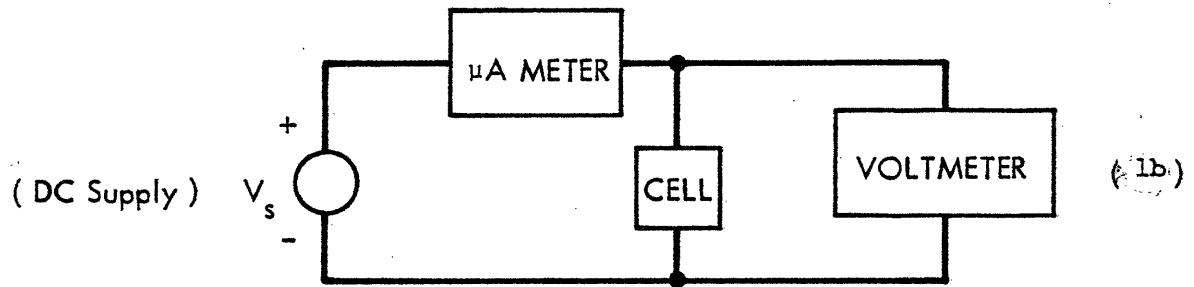
C.1 Circuit for Direct-current V-I Measurements

In circuit 1a, the series resistance, R_s, is chosen much smaller than the cell impedance, so that "Voltmeter 1" measures cell current, with only a minimal effect on cell voltage. We note, however, that if the cell generates its own current under these conditions, it will also experience very small voltage fluctuations, which are undesirable. The variant circuit 1b may also suffer from a drifting potential drop across the µA Meter (or electrometer).
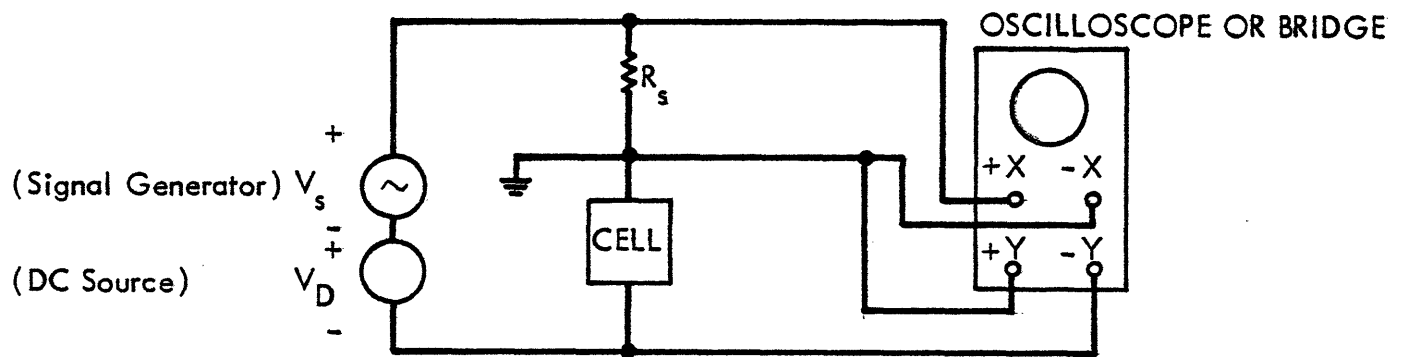
C.2 Circuit for AC Impedance Measurement

(DC Supply) V_s (1a)

or

(DC Supply) V_s (1b)
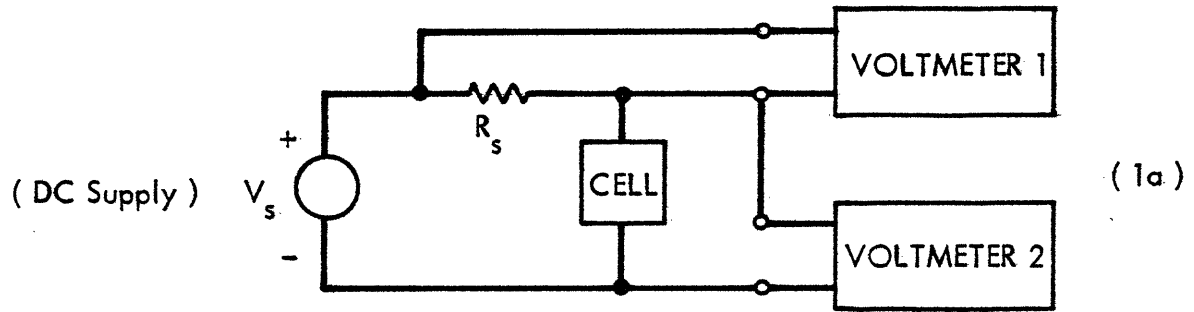
C.1 Circuit for Direct-current V-I Measurements

C.2 Circuit for AC Impedance Measurement

This circuit is essentially the same as circuit 1, except that the grounding configuration may be important, and provision may be made for adjusting the DC bias (V_D) if necessary. In general a dual-trace or a Lissajou pattern gave the most satisfactory measurements. In determining phase angle, tuning of probes and equivalence of x and y sweep circuits on the scope is important.

C.3 Circuit for plating

In electroplating, each cell electrode was successively grounded, while a DC voltage was between it and a piece of bare silver inserted into the fill hole, exactly midway between the electrodes. Current was measured by a series mA-meter. The unused electrode was disconnected.

C.4 Other Circuits

The Trygon power supply provides for added voltage regulation by means of reference sensing leads, as shown below
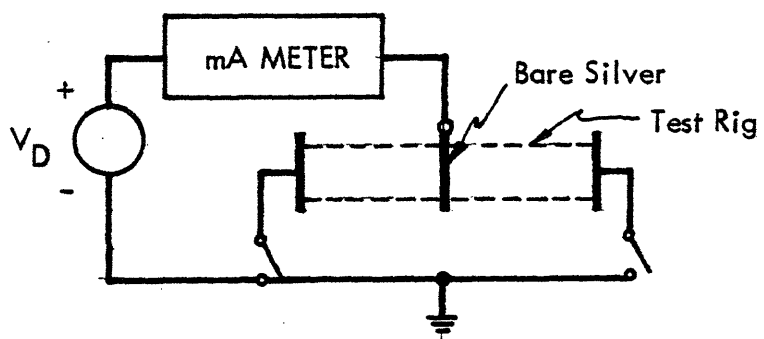
C.3 Circuit for plating
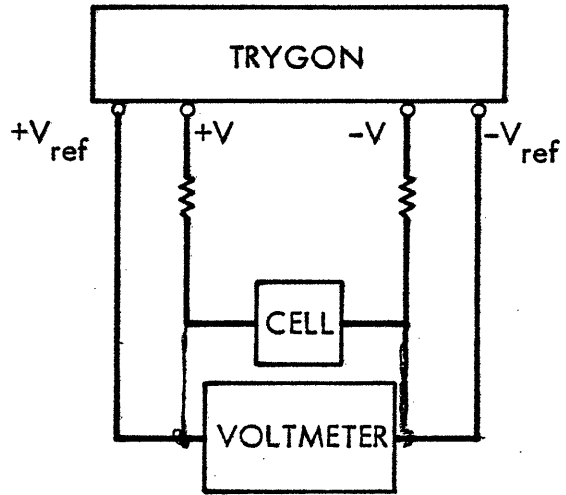
C.4 Other Circuits

Circuit 5

An alternate constant-current circuit for measuring cell impedance relies on a parallel-resistance combination

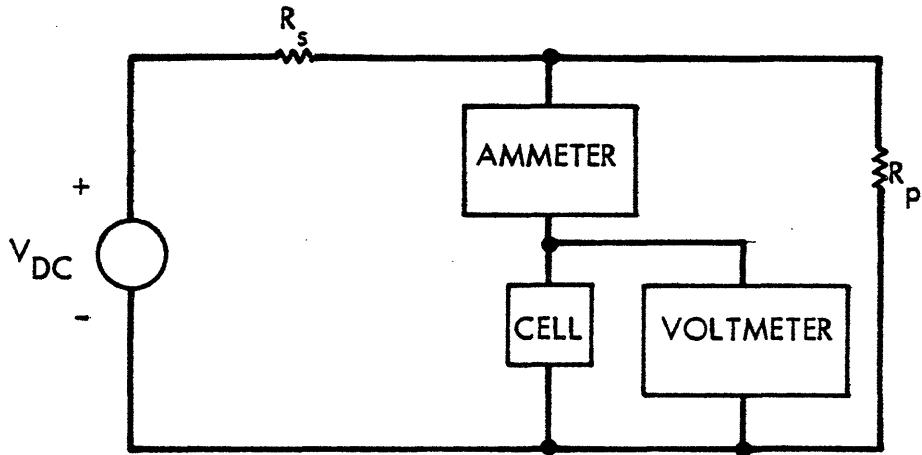where R_p is much less than the cell resistance and R_s is larger. This circuit has the potential disadvantage that since the cell resistance may be moderately small, the resistor R_p might have to carry a significant current.

III. <u>Summary of Experiments</u>

<u>Experiment A</u>: Plating Experiments

(1) Purpose: To examine qualitatively the various compounds which can be electrodeposited on silver in NaCl solution.

(2) Procedure: A third polished silver electrode is placed in the center orifice of the test-rig. This is used as the cathode with each end electrode successively used as the anode. Direct current was applied at prescribed current levels for various periods of time. Solution concentration about .05N NaCl.,pH approximately 7.0. Tests were made under conditions of subdued daylight plus indirect fluorescent lighting. Ambient temperature (65-85°F) and pressure (1 atm.) were not specifically controlled.

(3) Observations: The following observations were made on several sets of electrodes in the course of other tests.

(a) After (.6ma x 240 sec.) at each anode, an <u>opaque yellowish</u> coating was obtained. In the course of experiment B (following) DC currents of up to ± 7 ma were applied between the end electrodes for a period of approximately 36 min. Following this procedure, the electrodes had a dark brown coating.

(b) On fresh electrodes (12 ma x 120 sec.) produced small <u>dark spots</u> on a yellowish background. An additional (0.6 ma x 600 sec.) produced a <u>thick, plum-colored coating</u> which rubbed off easier than the yellowish coating.

(c) In another experiment, (.6 ma x 3600 sec.) produced an even, <u>very light coating</u> on one electrode and uneven dark spots on the other. An additional (3 ma x 1500 sec.) on the spotted electrode produced an uneven coating forming along lines where the electrode had been polished. A
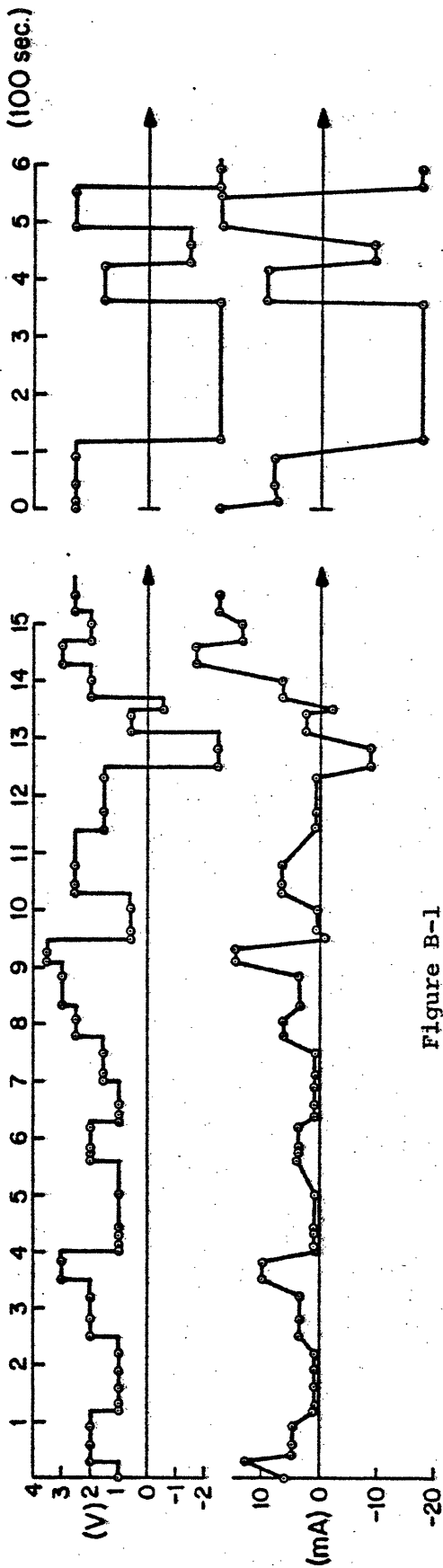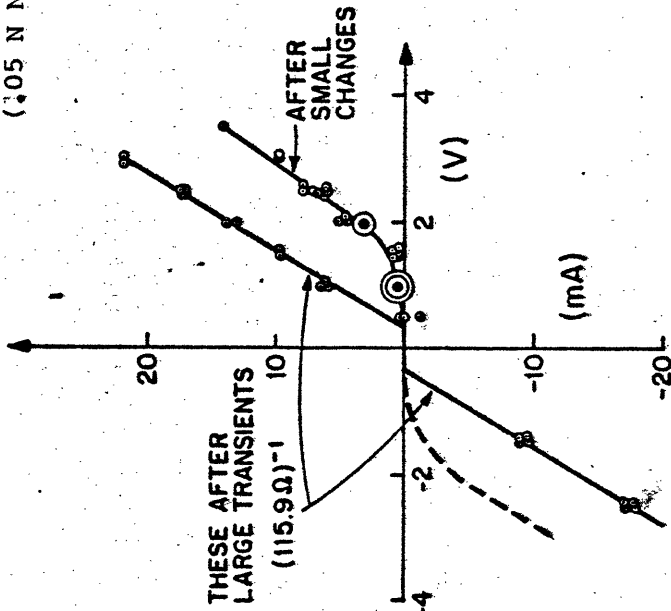
Figure B-1
V-I, PLATED ELECTRODES
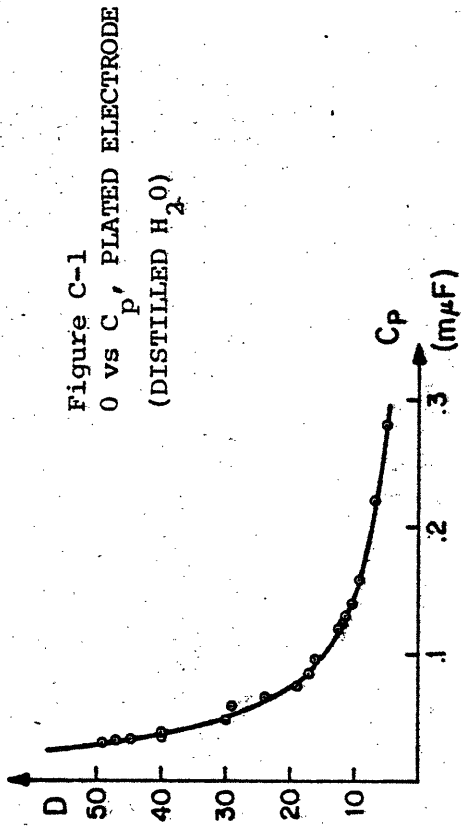(.05 N NaCl)

Figure C-1
0 vs C_p, PLATED ELECTRODE
(DISTILLED H_2O)

Figure B-2
V-I, PLATED ELECTRODES (.05N NaCl)

further (3 ma x 2100 sec.) produced an even, <u>dark brown coating</u>. (30 sec x 600 ma) produced extremely rapid <u>gas evolution</u> at the (bare) cathode and slower but significant gas evolution at the anode. The anode ends with a <u>thick white coating</u>.

(d) In another experiment (780 sec. x 25 ma) in a moderate concentration of <u>HCl</u> produced an adherent, even dark brown coating. The quality of this coating appeared more uniform and durable than that obtained in NaCl solutions. Janz and Ives also recommend coating in HCl—though at much higher currents and concentrations.

<u>Experiment B</u>: Preliminary VI Relation of Plated Electrodes

(1) Purpose: Obtain preliminary parameters for VI curves using test rig.

(2) Procedure: Curcuit (1b) was used. 0.05N NaCl solution was used. Electrodes were previously plated (240 sec. x .6 ma) individually using procedure of Experiment A, case (b).

(3) Observations: Figures B-1 and B-2 show voltage and current vs. time, and voltage vs. current, respectively, for applied voltages between .5-3.5 V. Step changes in voltage (0.5 to 1.0V in amplitude) produced a simple overshoot transient (2-5 sec. duration) in current. Voltages were sufficiently high that plating and gas evolution occurred during the experiment. The plating process is non-reversible, in that anode becomes dark brown during the test, while reversing polarity causes new anode also to become dark brown without significant change in color or appearance of original anode. The approximate impedance (figure B-2) was 116 Ω.

<u>Experiment C</u>: Bridge Measurement (Chlorided electrode, distilled water)

(1) Purpose: Test commercial impedance bridge (GR Type 1650A) for measurement of cell impedance.

(2) Procedure: The bridge uses an internal 6V. source for measuring DC resistance and a 1KHz internal source for AC measurements. The electrode coating was dark brown; electrolyte was distilled water. The bridge is typically balanced by adjusting dissipation factor (D) versus parallel-equivalent capacitance (Cp).

(3) Observations:

(a) DC resistance was measured at 111.2KΩ.

(b) AC parallel-equivalent resistance was Rp = 111.2KΩ also. However, no single null could be obtained in measuring D and Cp; rather, a whole sequence of nulls was obtained, with the property $D \cdot Cp \approx 1.5$, x $10^{-9} \approx$ constant. (See Fig. C-1). Series-equivalent capacitance could not be measured due to the high dissipation factor. The null was deeper for higher D-values.

Experiment D: V-I Curve for Large Voltages (Chlorided electrode, distilled water)

(1) Purpose: Attempt to measure large-signal V-I relation with distilled water as electrolyte.

(2) Procedure: New silver electrodes with a dark brown coating (.6 ma x 240 sec.) were placed in distilled water after several rinses. Circuit (1b) with the Wavetek voltmeter and Data-precision digital ammeter were used.

(3) Observations: Figures D-1 and D-2 show current and voltage vs. time, and current vs. voltage, respectively. The V-I curve is approximately linear at about 92.5KΩ, in agreement with Experiment C. At a constant supply voltage, the current does not remain constant, but oscillates slightly with a very long period. Note that some plating may have occurred during this test.
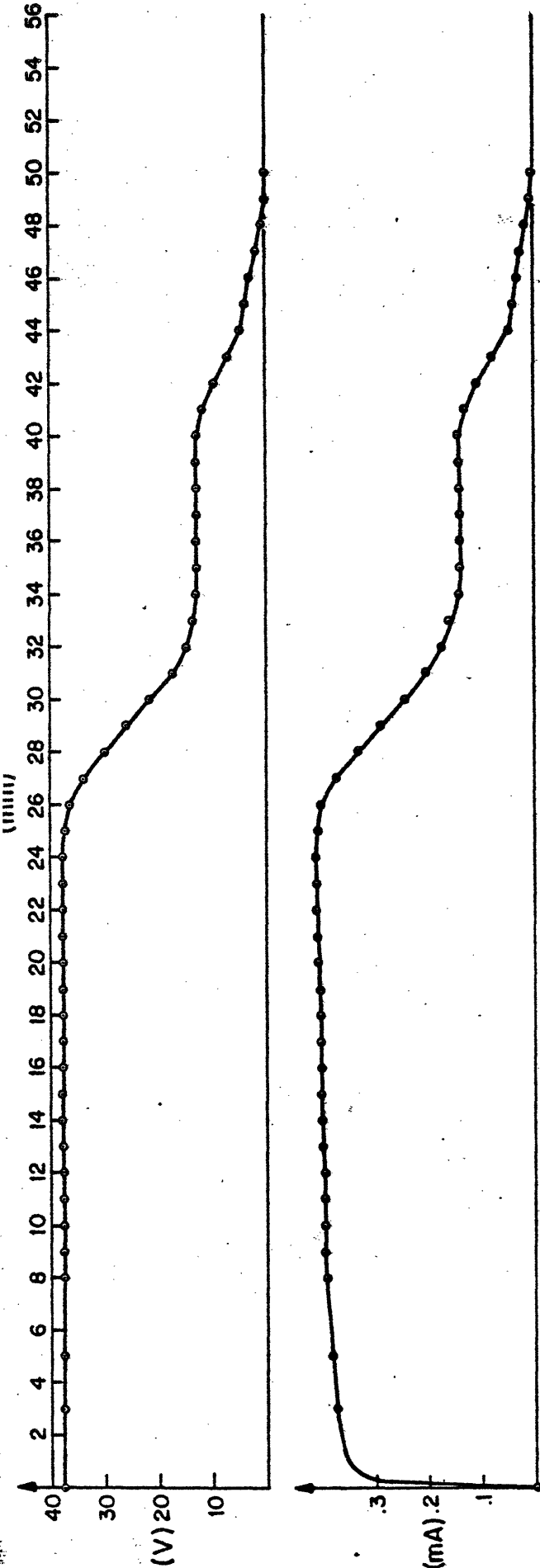
Figure D-1
V-I, PLATED ELECTRODES
(DISTILLED H_2O)
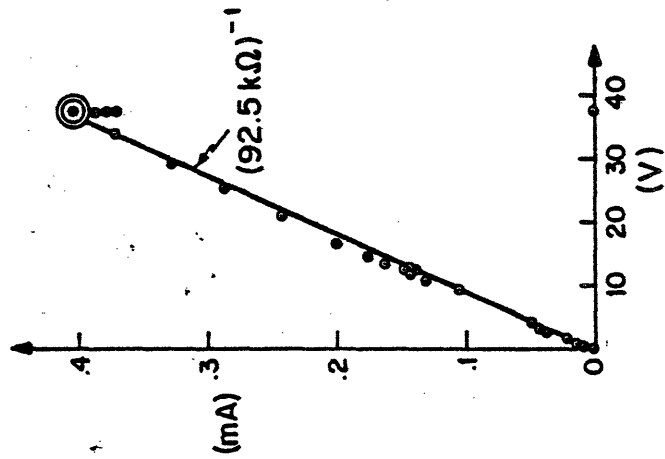
Figure D-2
V-I, PLATED ELECTRODES
(DISTILLED H_2O)

Experiment E: V-I Curve for Moderate Voltages (Chlorided electrodes,
.01N NaCl)

(1) Purpose: Measure dynamics and V-I Relation for moderate potentials.
Investigate stability of electrode at low voltages.

(2) Procedure: New silver electrodes with a dark brown coating (.6 ma x
240 sec.) were placed in .01N NaCl. A measuring circuit like 1(b) was
used.

(3) Observations:

(a) Measurement with impedance bridge revealed $R_p \approx 1.35K\Omega$, $C_p \approx 2.5 \times 10^{-9}f$.
at D = 50.

(b) Time-histories of V and I are shown on Figures E-1, E-2, and E-3.

(c) When the DC voltage exceeded .4V, a small fluctuation in the current
was observed. At 1.4V, the amplitude of this oscillation was about 30µA,
and the period about 20 minutes; this persisted over 2 1/2 hours of
observation. Current oscillation was observed from .4-1.65 VDC. [Later
tests using a battery as voltage source produced no oscillations, under
slightly different conditions.] See Fig. E-3.

Experiment F: V-I Curve for Higher Voltages (Chlorided electrodes,
.01N NaCl)

(1) Purpose: Investigate V-I Curve and plating effects at higher voltages.

(2) Procedure: Circuit (1b), with Trygon supply, Wavetek voltmeter, and
digital ammeter were used. The electrodes for this test were those used
in Experiment E. Electrolyte was also .01N NaCl.
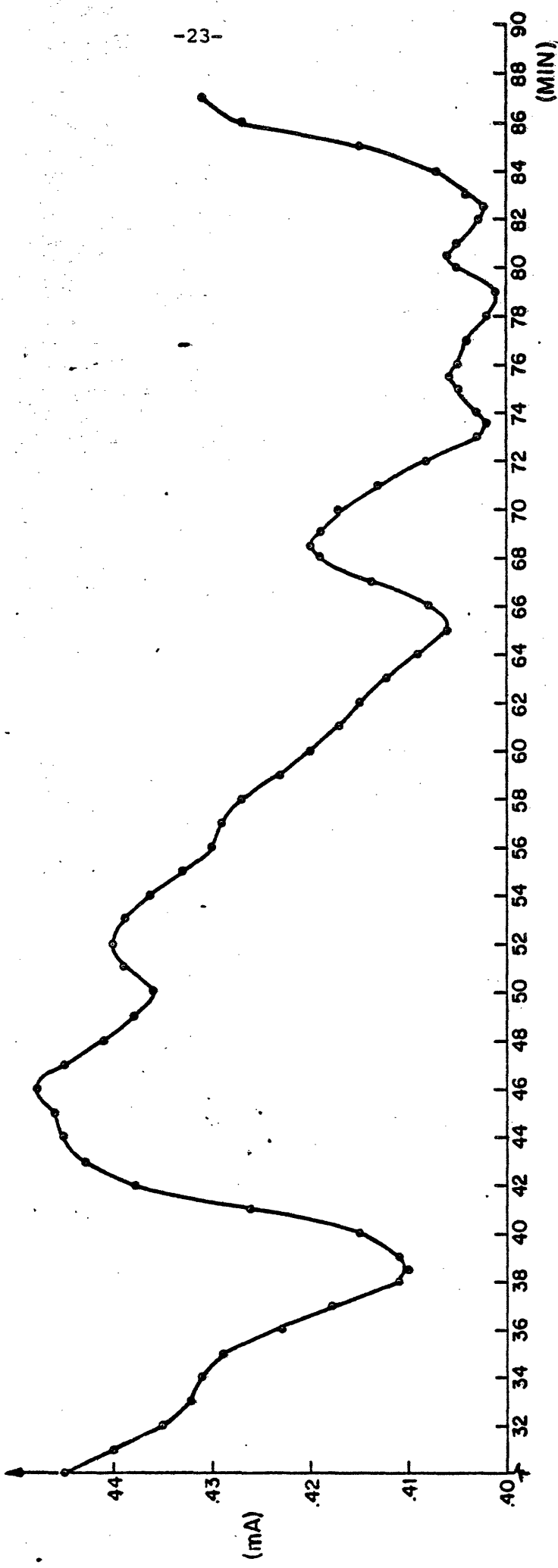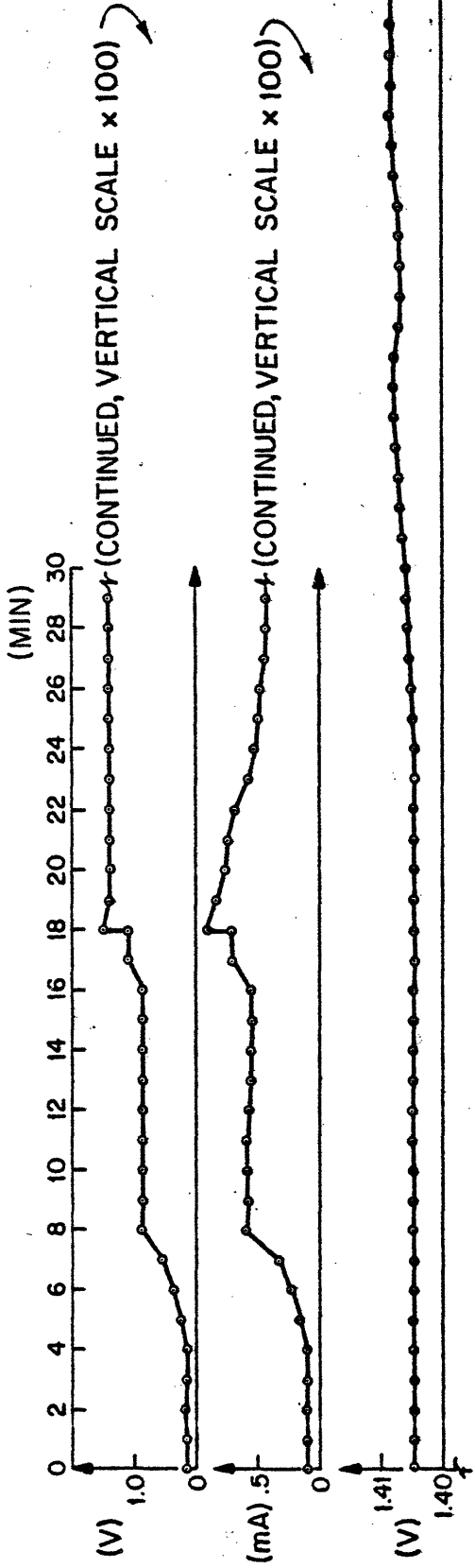
Figure E-1
V-I, PLATED ELECTRODE
(.01N NaCl)
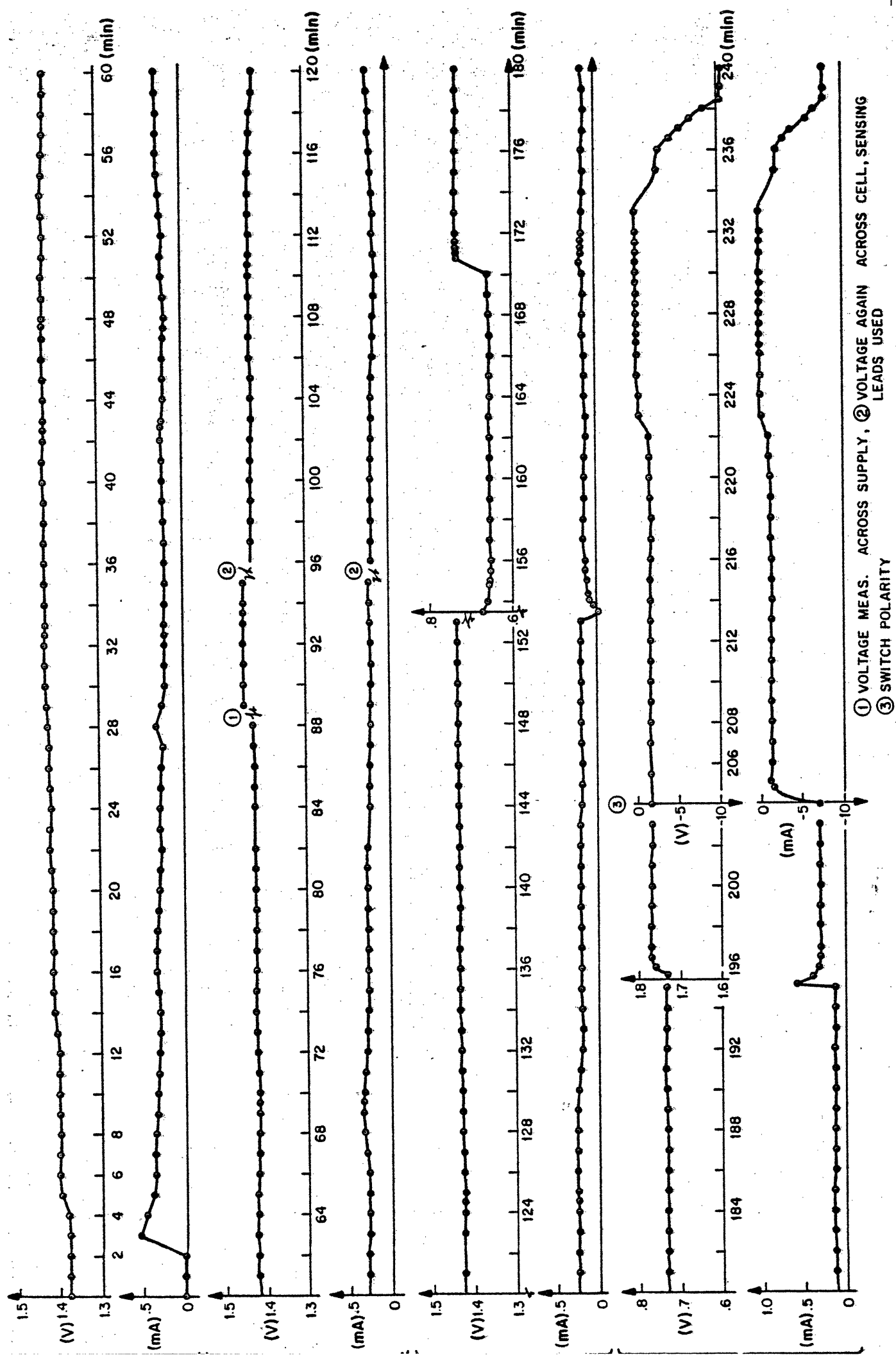
Figure E-2

V, I TRANSIENTS (PLATED ELECTRODES, .01N NaCl)

① VOLTAGE MEAS. ACROSS SUPPLY, ② VOLTAGE AGAIN ACROSS CELL, SENSING LEADS USED
③ SWITCH POLARITY
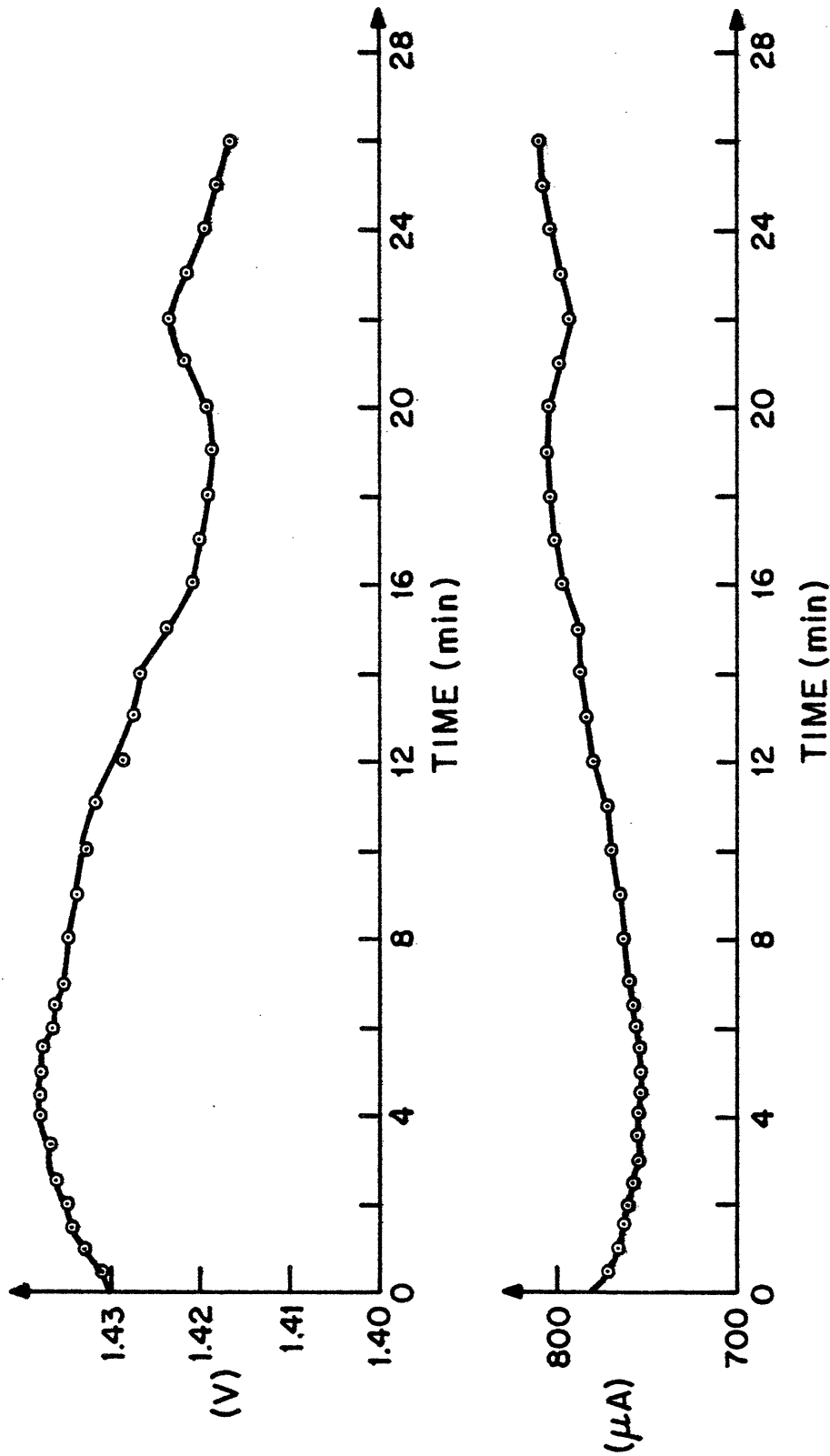
Figure E-3 V, I MICROTRANSIENTS (PLATED ELECTRODES, .01Na Cl)

(3) Observations:

(a) V-I data of Figure F-1 indicate a slope of .84 Ω.

(b) A gas evolves rapidly at the cathode at 40 VDC (500 ma). The cathode develops a chalky yellow coating. A profuse cloud of white translucent gelatinous substance is exuded from the anode and settles on the bottom of the cell. The anode develops a loosely-adherent lavender coating over a yellow coating.

(c) The cell was open-circuited and left undisturbed. After 48 hours the gelatinous substance became a purple sediment. pH of the original .01N NaCl was 6, the bulk solution after the tests above was pH7. Successively more concentrated samples of the sediment were pH10 and 12 respectively. The superinate changed from clear to brownish. This suspension did not settle significantly in 5 weeks and was partially settled after 7 weeks.

Experiment G: Affect of pressure

(1) Purpose: To determine the effect of hydrostatic pressure in the bulk solution on junction potential.

(2) Procedure: Bare silver electrodes were placed in .01N NaCl solution. A rubber stopper was placed in the inlet port of the test rig (not in contact with the bulk solution). The open circuit cell voltage was measured when the stopper was manually depressed. Recovery of open-circuit cell voltage after shorting of electrodes was also observed.

(3) Observations: The open-circuit potential increased from 2.3 to 2.7 mV when the stopper was pushed in. Probably due to the meter impedance, the cell voltage was decreasing from 2mV to 1mV. Pushing in stopper causes rapid decrease; substantial pressure caused a sign change to -4.9mV. See Figure G-1, for transient response to electrical short-circuit.
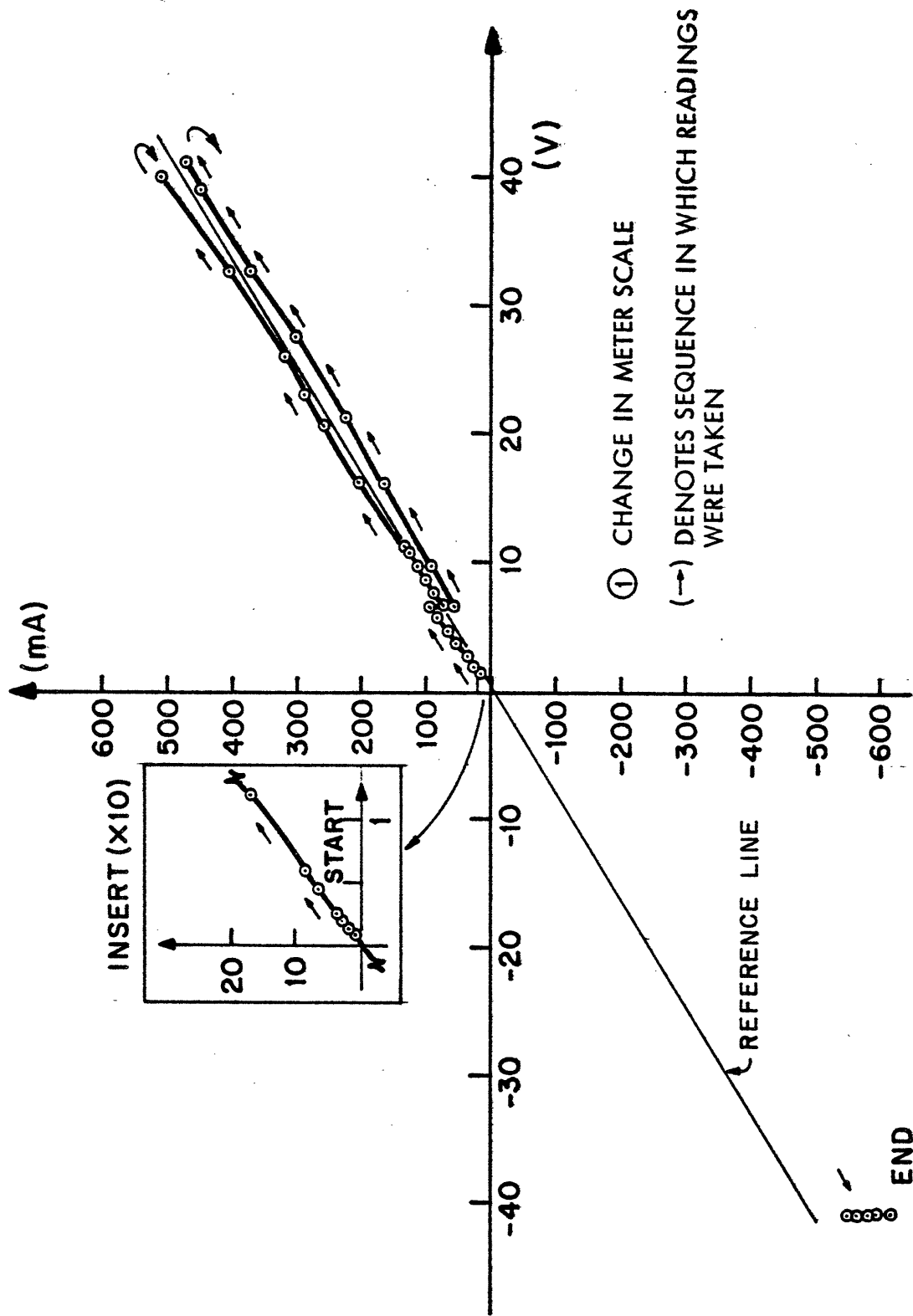
Figure F-1

LARGE-AMPLITUDE V-I RELATION
(PLATED ELECTRODES, .01N NaCl)
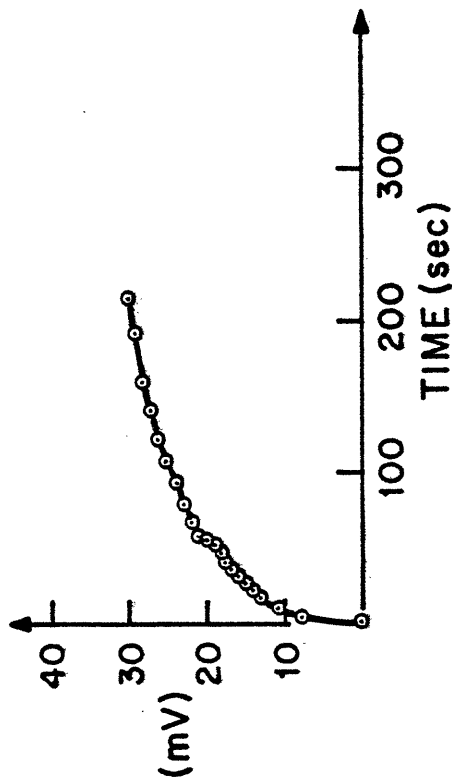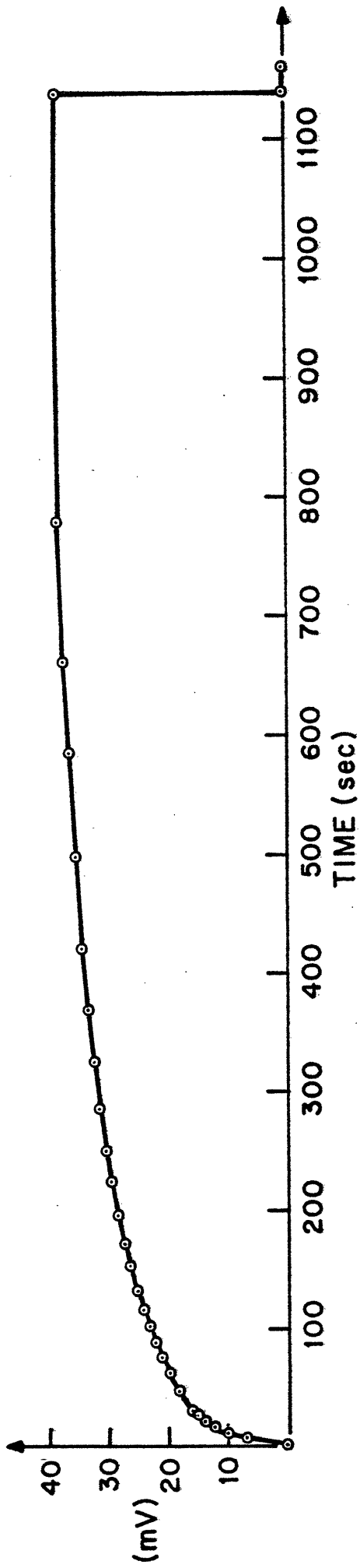
Figure G-1

OPEN-CIRCUIT CELL VOLTAGE AFTER SHORT
(BARE ELECTRODES, .01N NaCl)

Experiment H: Microporalization Studies (bare silver, .01 N NaCl)

(1) Purpose: To determine micropolarization (low-voltage V-I) curves, which are useful in estimating reaction parameters.

(2) Procedure: Bare silver electrodes (from Experiment G) in .01 N NaCl solution were used. A 100KΩ resistor was used in series with the Trygon supply, along with sensing leads and external programming resistor, in a modification of circuit (1b). The HP425A μ-ammeter and Wavetek precision voltmeter were used.

(3) Observations:

(a) The current-voltage relationship was quite nonstationary (Fig. H-1).

(b) Cell current was observed to exhibit micro-oscillations; these were not observed when the test cell was replaced by a resistor.

Experiment I: Continuation of Experiment H

(1) Purpose: See Experiment H

(2) Procedure: "   "   "

(3) Observations: A supply voltage and cell current were increased. When the current reached .09 mA, the cell voltage rose on its own. When cell voltage reached 400 mV (from 100 mV), the supply polarity was reversed by means of a crossover switch. Current then went approximately to zero, while cell voltage came transiently from -135 to -20 mV.

Experiment J: Micropolarization Studies (bare silver, .1N NaCl)

(1) Purpose: See Experiment H.

(2) Procedure: "   "   "
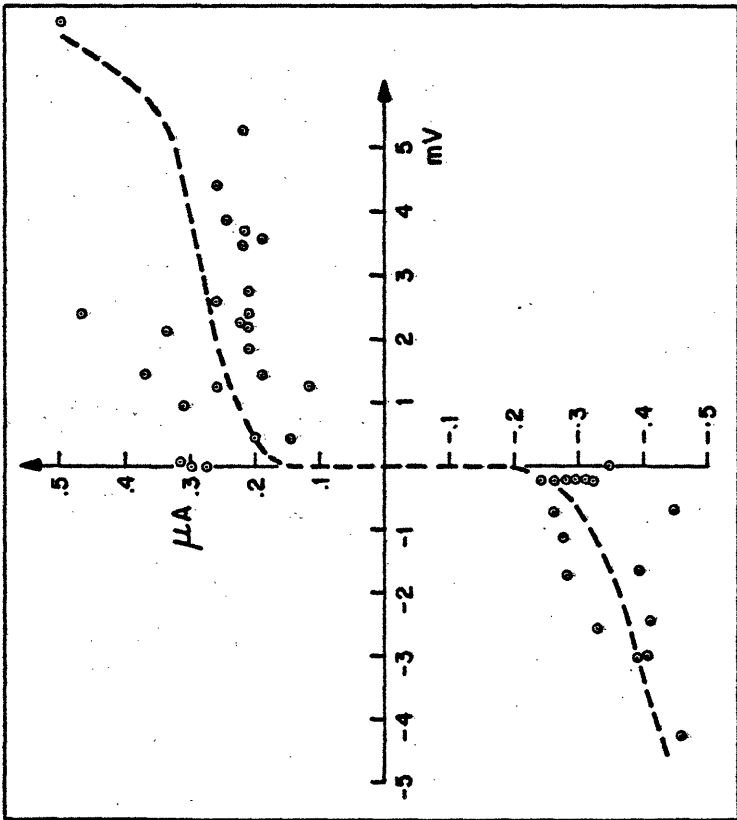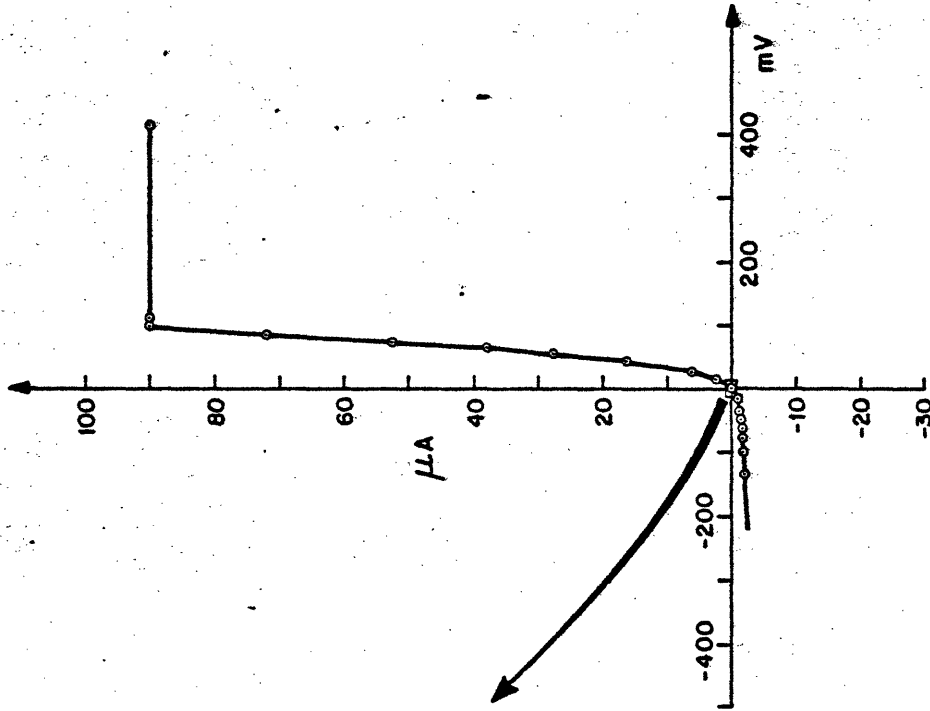
Figure H1

MICROPOLARIZATION CURVE (BARE SILVER, .01N NaCl)

(3) Observations: Results similar to Experiments H-I.

Voltage runaway effect was observed again.

Experiment K: Micropolarization Studies (plated electrodes, .01N NaCl)

(1) Purpose: See Experiment H.

(2) Procedure: Same as Experiment H, except that each electrode was

plated 35 min. at 3ma., giving a uniform dark brown coating.

(3) Observations:

(a) V-I relation of Fig. K-1, up to 200 mV, showing an impedance of about

560 Ω.

(b) Cell currents were stable and exhibited no unusual transient behavior,

even at low voltages. "Hysteresis" effects (i.e., repeatability) was to

within 10 mV in a 200 mV curve.

Experiment L: Micropolarization Studies (plated electrodes, .1N NaCl)

(1) Purpose: See Experiment H.

(2) Procedure: Same as in Experiment K.

(3) Observations:

(a) V-I relation of Fig. L-1, showing impedance of about 50Ω.

(b) Similar to observations of (b) above.

Experiment M: AC Impedance Measurements

(1) Purpose: To determine impedance of Ag/Ag Cl electrodes under

various conditions.

(2) Procedure: Circuit (2) was used. A series resistor of 1234Ω was

used to measure current. The peak-peak cell voltage in all cases was .2V.

At very low frequencies an HP Model 202A signal generator was used; at audio

frequencies the HP Model 200CD was used. Dual-trace and Lissajous patterns
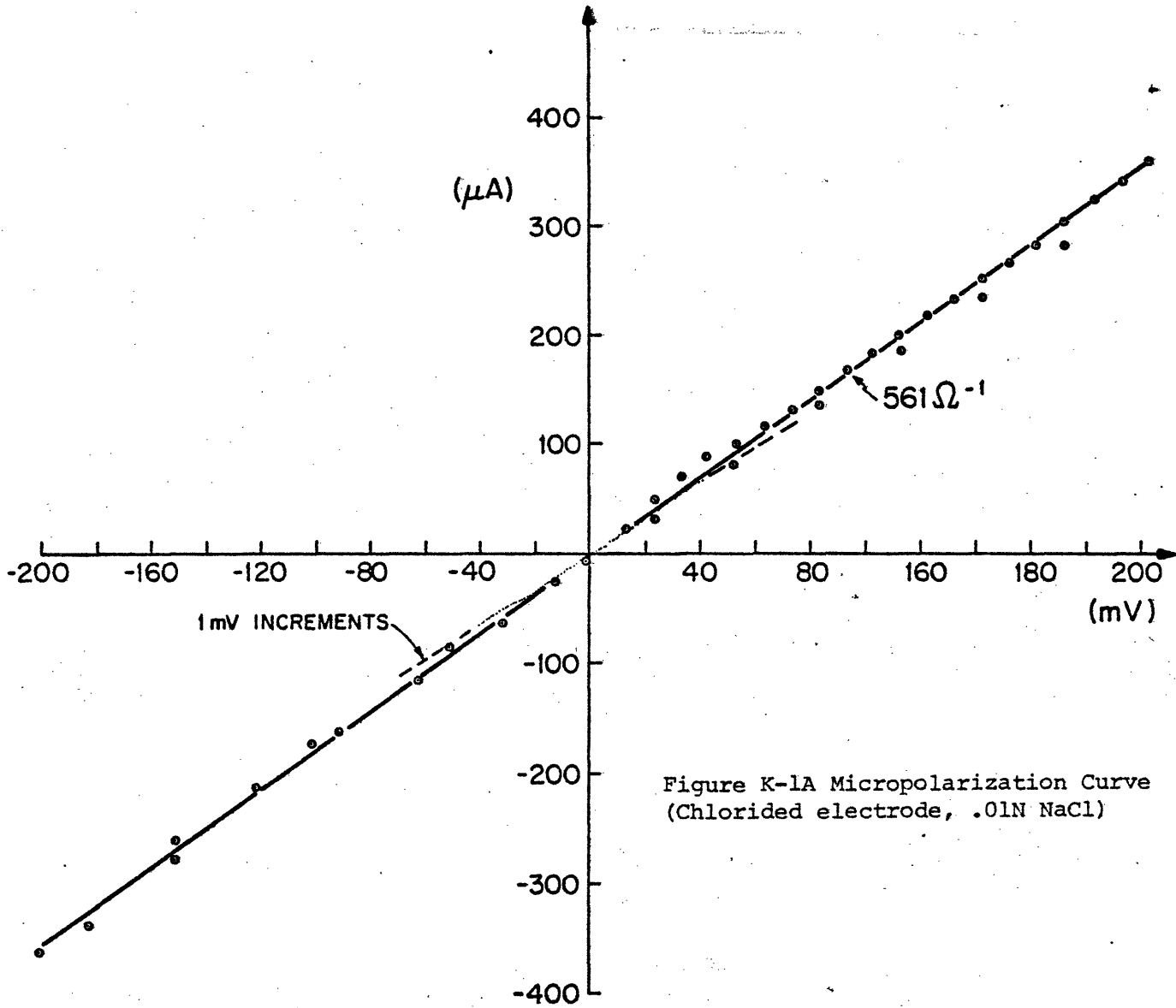
Figure K-1A Micropolarization Curve
(Chlorided electrode, .01N NaCl)
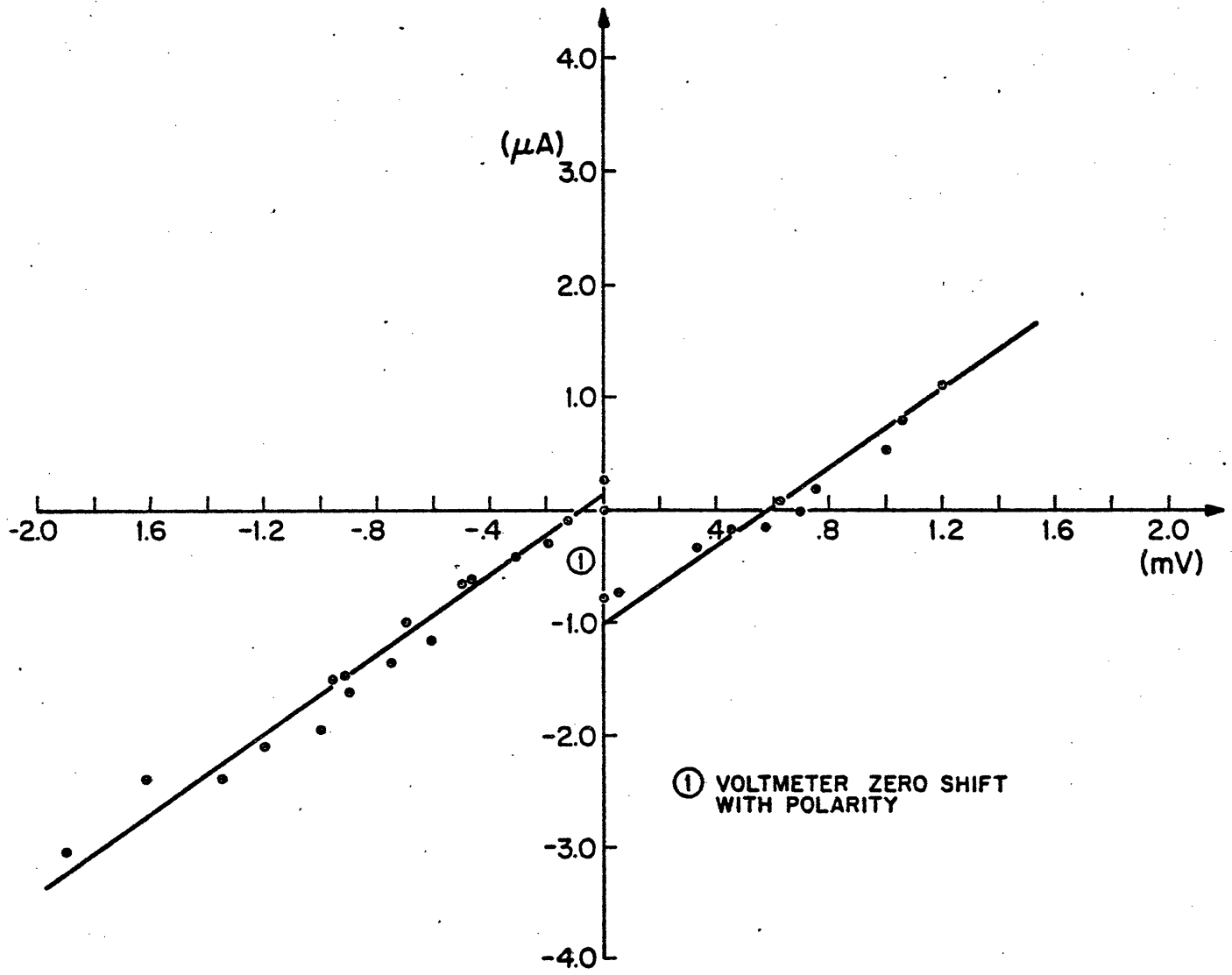
Figure K-1B MICROPOLARIZATION CURVE
(Chlorided electrode, .01N NaCl)
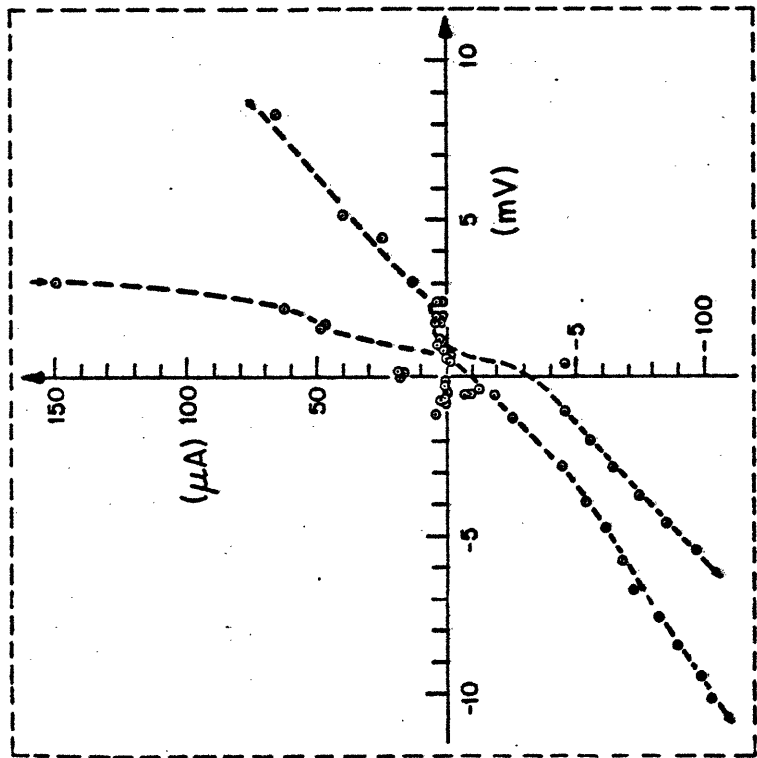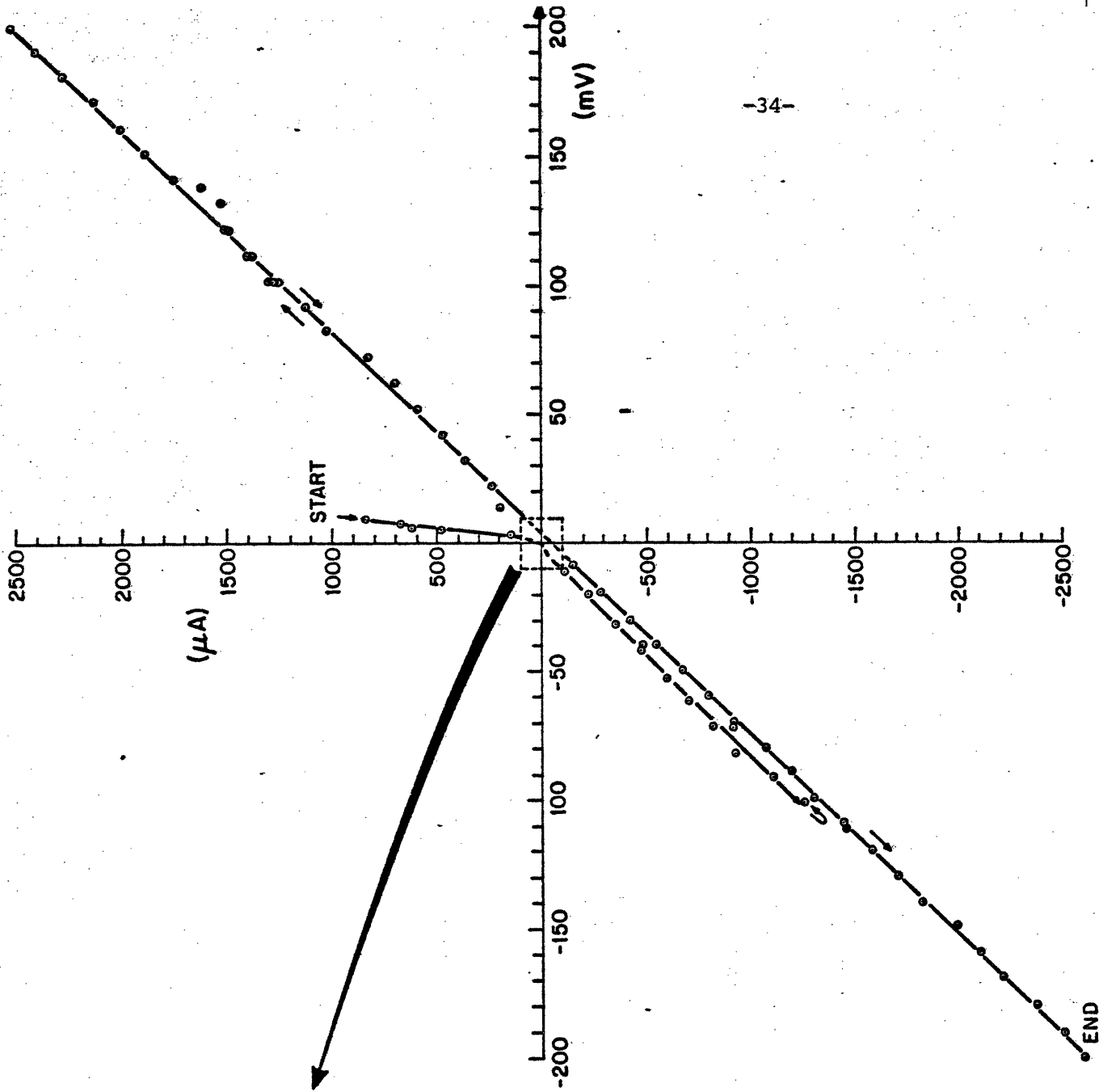
Figure L-1
MICROPOLARIZATION CURVE
(PLATED ELECTRODE, .1N CaCl)

gave approximately equal impedance estimates. The value of series resistance was found to affect slightly the measured cell impedance, probably due to loading of the Model 202A.

(3) Observations:

(a) Figures:

   M-1: No plating, .01N, NaCl

   M-2: No plating, .1N NaCl

   M-3: Plated, .01N NaCl

   M-4: Plated, .1N NaCl

(b) A spectrum analyzer revealed no harmonics generated by chlorided electrodes.

Experiment N: Effect of Voltage on AC Impedance

(1) Purpose: To determine effect of peak-peak voltage on cell impedance measurements.

(2) Procedure: Circuit (2) was used. Impedance curves were run for 12V pp and .04V pp across the cell. Procedure otherwise as in Experiment M.

(3) Observations:

(a) See Figures N-1, N-2.

(b) The GR bridge did not agree with dual-trace and Lissajous measurements.
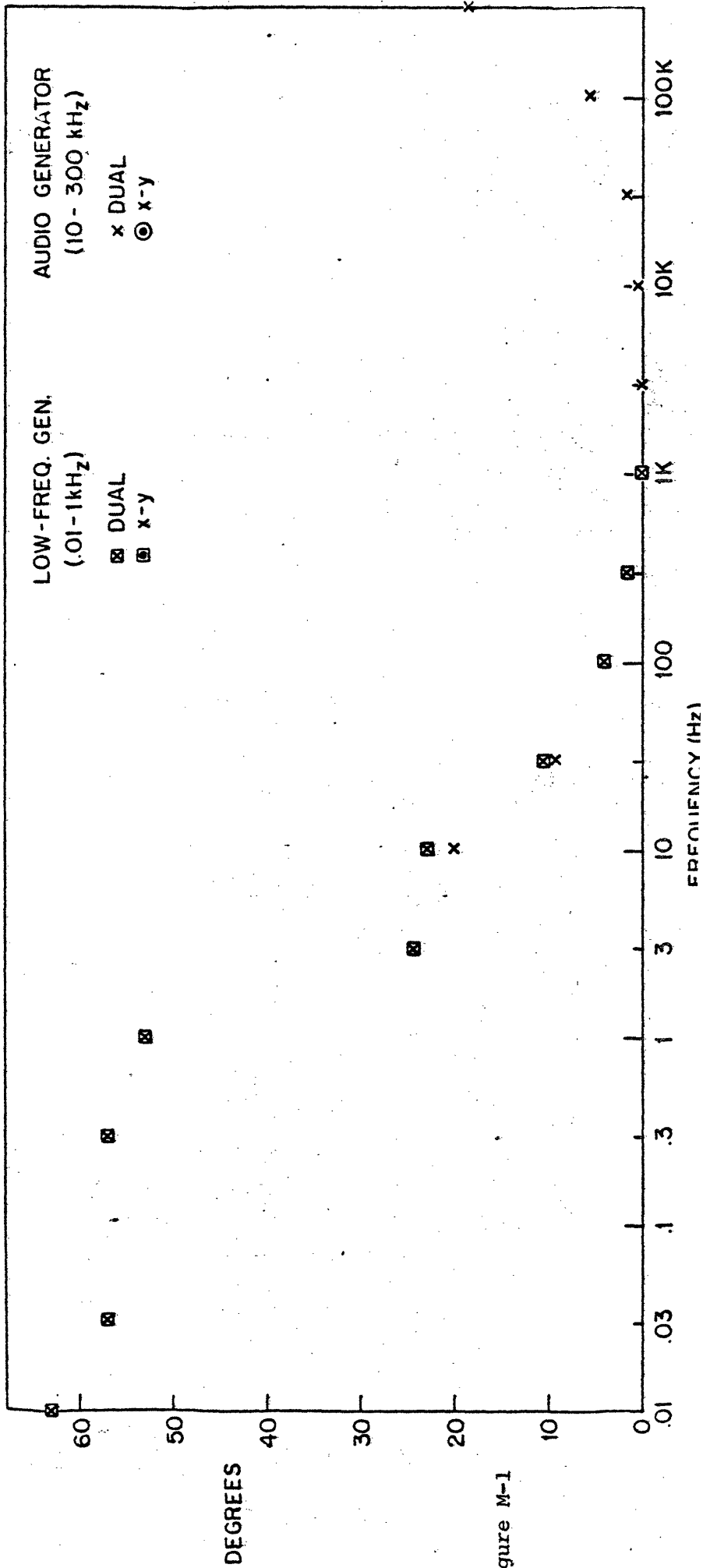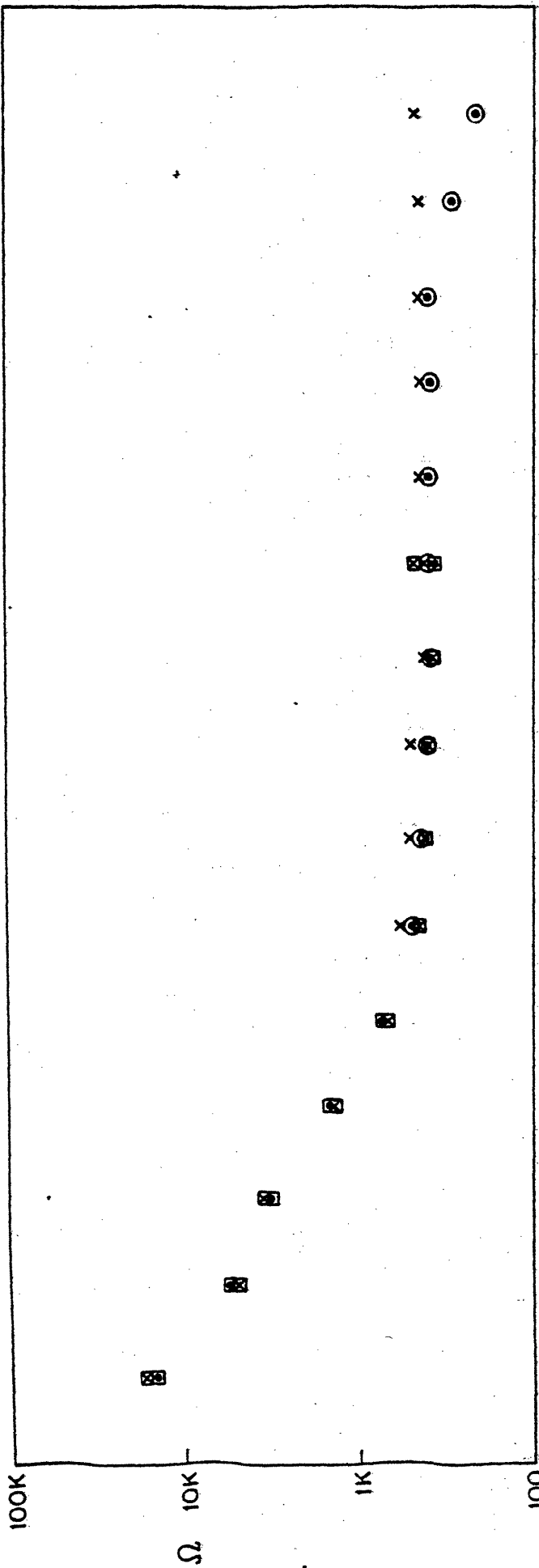
Figure M-1
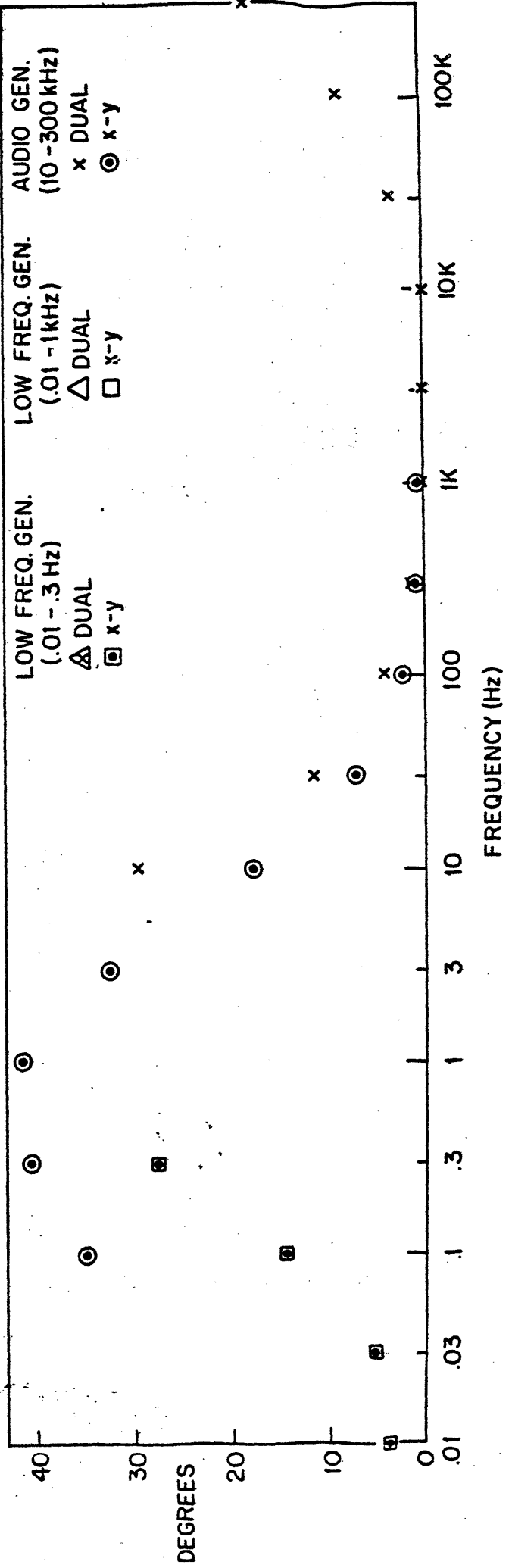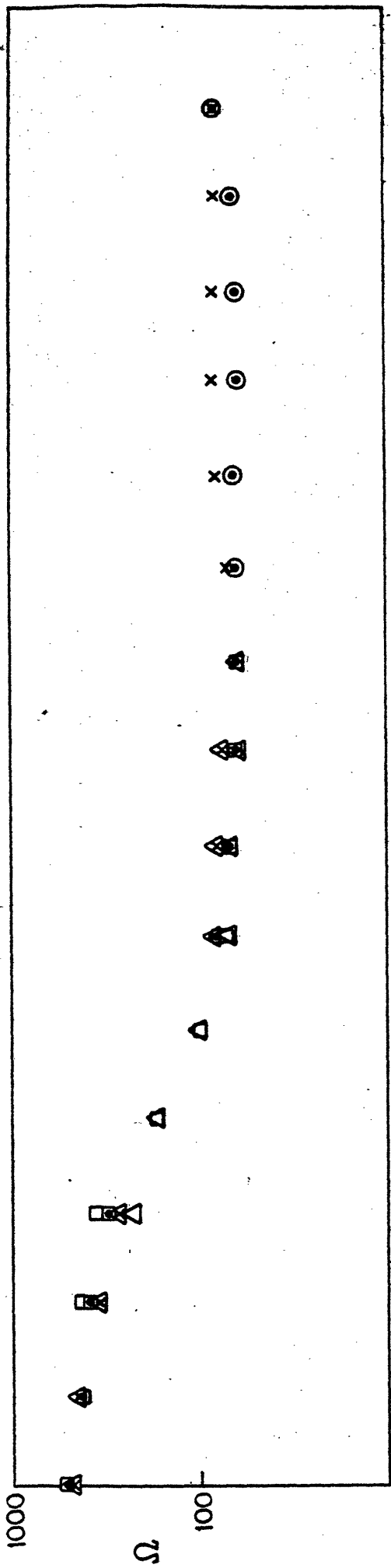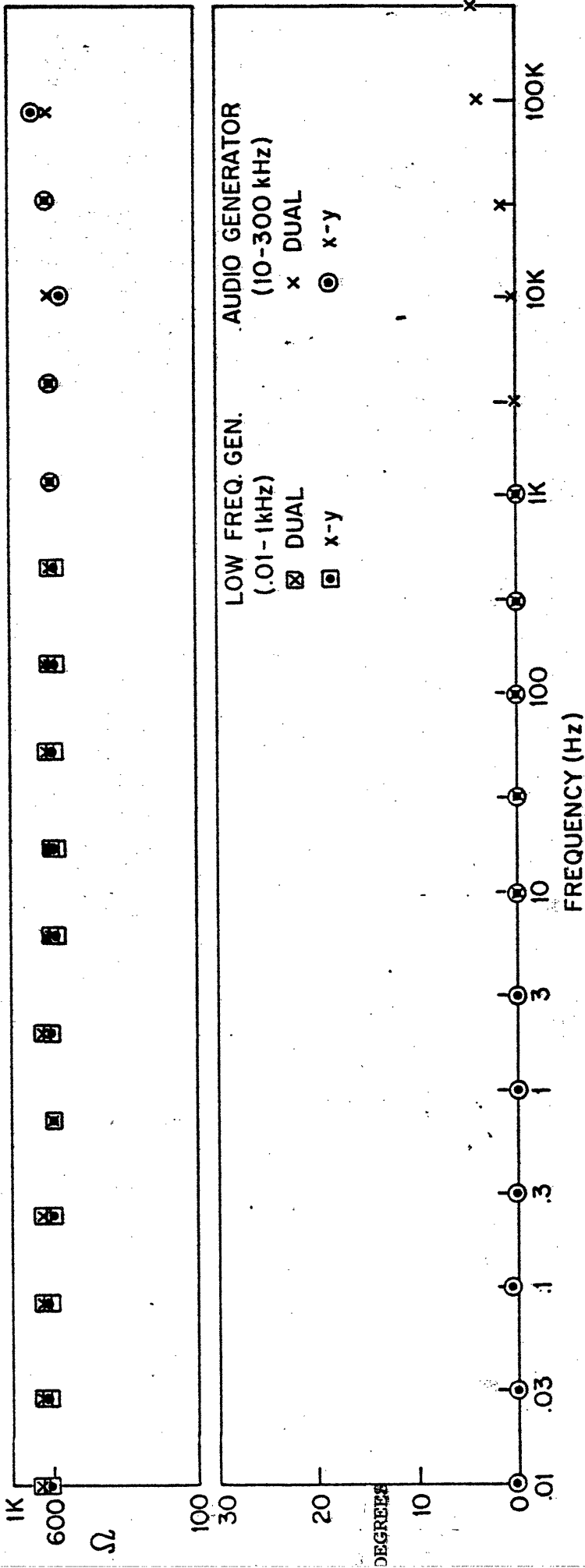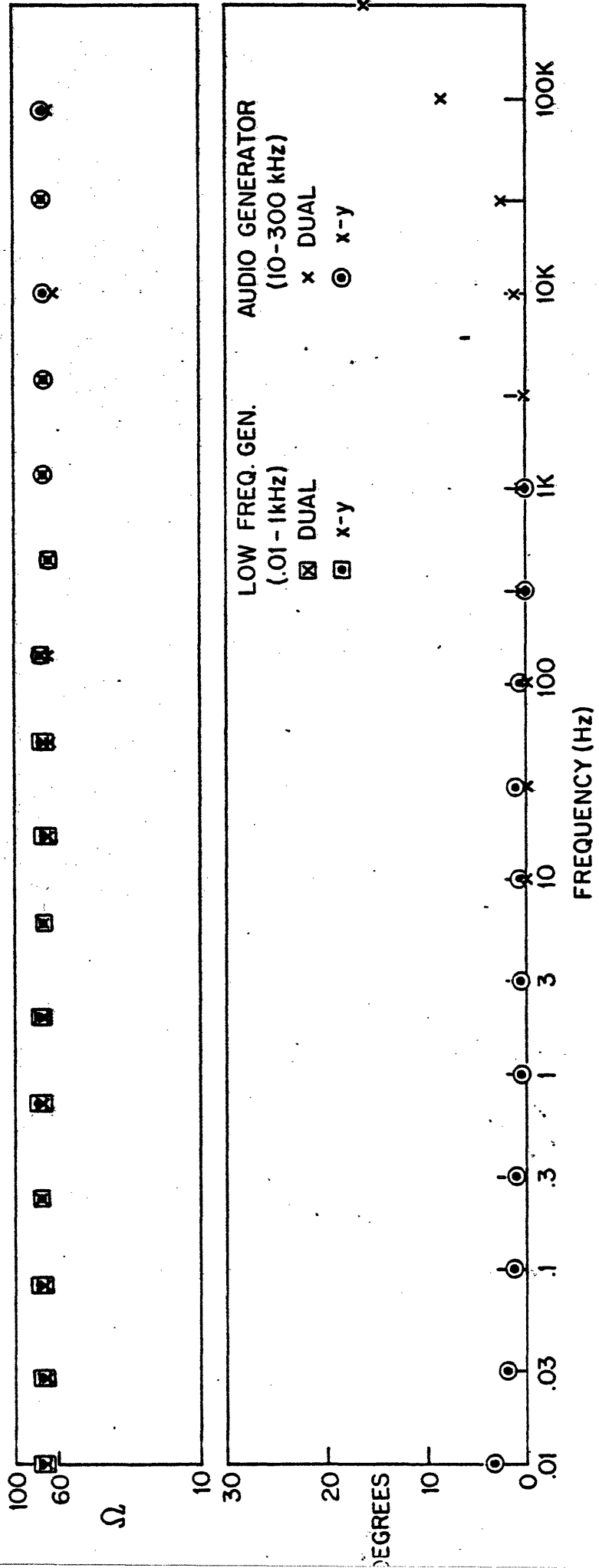
Figure M-2

Figure M-3

Figure M-4

IV. Discussion and Conclusions

Casual observation of electrode properties, particularly when conventional circuit-measurement techniques are employed, is likely to be misleading. The data clearly indicate that the static and dynamic properties of $Ag/AgCl_s$ electrodes are much more complex than normally supposed, and that the effects of these properties are apparent even in the normal operating range of such electrodes. While the qualitative conclusions outlined below are based on data from single electrode pairs (our experiments being limited by the cost of silver and the preliminary nature of our studies), they are consistent, and are in many cases borne out by supplement experiments which we have not documented in this report. We proceed to summarize some of the physical effects which our experiments thus far have indicated to be significant.

Irreversibility of electrode phenomena: Static and dynamic behavior of electrodes in an immediate experiment depends in detail upon the <u>entire past history</u> of the electrode, at least from the time that the electrode metal was first exposed to a solvent. This observation calls into question the very concept of "physical properites" of an electrode, in the sense that repeated trials of an experiment may not yield the same estimates of physical parameters (e.g., as in estimating an "equivalent circuit" for an electrode). Probably the most relevant measures of the past history of an electrode (i.e, those necessary to predict its future performance) are the amount and type of all chemical compounds deposited on the electrode surface. We have been quite careful, for this reason, to design our experimental sequences: typically open circuit measurements and micropolarization experi-

ments for bare silver might precede plating, and then open circuit micro-
polarization, and low-level AC measurements for plated electrodes would
precede higher-voltage AC and DC measurements, respectively. Note the
dual presentation of time-histories and V-I Plots in several instances.
It is evident from experiments A and F that electrode reactions are not
reversible: reversing applied potential does not merely reverse chemical
reactions. The common practice of shorting electrodes to reduce junction
potentials may also be questioned, as it assumes at least a sort of local
reversibility of the cell reactions.

Many forms of $AgCl_{(s)}$ (?): Compounds observed to form on the electrodes
may be distinguished by color (yellow, brown, purple, white, transparent)
and by hardness (respectively plaquelike, powderlike, scaly and gelatinous).
The above compounds are listed in order of decreasing adherence to the silver.
In future experiments we anticipate chemical analysis of some of these sub-
stances. On the basis of similar observations by other investigators, it
is possible that all of these compounds represent various forms of $AgCl_{(s)}$,
but oxides and oxychlorides (etc.) of silver cannot be ruled out. Temper-
ature, pH, and exposure to light, as well as applied potential, will affect
the plating process and stability of the plated compound. When electrodes
are used for recording, the most stable and adherent coating would generally
be preferable. The yellow coating could be obtained at low plating rates
in HCl or NaCl. A flaky white coating, usually accompanied by evolution
of gas (probably H_2, or O_2) was obtained at higher plating rates. As applied
potential is increased, additional chemical reactions become feasible,

additional unstable compounds may be formed, and the ion concentrations of the bulk solution may be significantly affected. We do not believe chemical impurities account for any major features of our observations. Certainly, definition of possible reaction mechanisms (by literature search and/or independent experiment) is crucial to the next phase of this research.

Static electrode behavior: No electrode pair exhibited perfectly repeatable near-DC behavior (within the accuracy of our measurements), and hence no truly "static" properties can be asserted. The data from plated electrodes in a concentrated solution (.1-.5N NaCl) were most nearly repeatable. We shall thus discuss approximately-static behavior.

Static behavior of bare silver electrodes in dilute solutions (Expt. H) show greatest non-linearity. Our observations of a micropolarization current (Fig. H-1) which switches abruptly with potential, is not believed to be due to meter characteristics, and is at variance with commonly accepted theory (see Thirsk and Harrison, Ch. 1). At present we have no explanation for the observations of Experiment H, though this type of experiment is potentially valuable in elucidating reaction mechanisms. Further experiments are under way. Plated electrodes in distilled H_2O (Expt. D) show a finite impedance which may be attributable to H^+ concentration (see below). The trend of the current to increase (Fig. D-1) when potential is held constant for several minutes may be attributable to the transport of ions (Ag^+, A^+, OH^-) into solution due to surface reactions.

The rate of recovery of the junction potential after bare electrodes are shorted (Fig. G-1), or after a change in pressure, gives an indirect

measure of reaction rate and/or diffusion rate. A "time constant" on the order of 100-200 sec. is apparent, although the recovery is evidently <u>not</u> of the simple exponential form. When data is measured quasistatically, allowance is made for this long-term behavior. Analagous time constants for plated electrodes and/or more concentrated solutions are much shorter, however.

Several electrode pairs (Experiment E) revealed a curious tendency of the current to exhibit micro-oscillations with periodicities of 5-30 min. when the voltage was held nearly constant at certain values. When this occurred, the current oscillations were out of phase with the (very much smaller) voltage variations, indicating a <u>very localized negative-resistance region</u> on the V-I curve, so small as to be indistinguishable on a normal-plotting scale. We conjecture that this may be due to a <u>buffering</u> effect of competing chemical reactions. For plated electrodes in .01N NaCl, this was observed around 1.41 volts. The data of Experiment L appear to suggest similar effects at 1.5 mV and 130 mV in .1N NaCl, although these were not fully investigated.

Most of the V-I curves for plated electrodes exhibit a long-term <u>hysteresis</u>-like effect, in that currents recorded during increasing voltage sequences are typically larger than currents recorded during decreasing voltage sequences (Expt. B, K, L). Step voltage changes often elicit brief current overshoots (Fig. B-1) which decay within a few seconds for plated electrodes. The data of Figure B-1; when plotted in V-I format, (Fig. B-2) appear to cluster along two curves, points of the lower (nonlinear) curve

occurring with small ($\leq$ .5V) changes in potential, and points of the higher (linear) curve being tabulated for large changes in potential ($\geq$ .5V). We do not fully understand this phenomenon. The data of Figure K-1A perhaps indicate a similar trend; slope of the 200-mV curve taken at approximately 10-mV increments is very slightly greater than that of the 40mV curve taken at approximately 1mV intervals (dotted line in Figure).

Threshold potentials for quasireversible reactions encountered for these electrodes, manifested as rapid increase and decrease in slope of the micropolarization curve, are known to be very small and difficult to measure (Thirsk and Harrison, Janz and Ives). Our data are not sufficently precise to demonstrate such effects conclusively, though we note possible threshold potentials in Figures H-1 (at 5 mV) and L-1 (at 1.5 and 130 mV).

The most striking feature of the several polarization curves is their approximate linearity over a wide range of voltage values—even during the occurrence of rapid plating and gas evolution. The apparent DC resistance of the electrode pair in solution depends strongly on concentration of ions in the bulk solution. We have the following data:

Experiment	Concentration (N, NaCl)	Resistance (Ω)
D	0	10^5
K	.01 $\bigg\}$ (c_s)	560 $\bigg\}$ (R)
L	.1	80

We postulate an empirical relation of the form

$$R = R_e + R_s (c_o + c_s)^{-1}$$

where we expect R_e to denote the DC resistance of the electrode junction, R_s the resistance (per electrode area) of a solution having one normal-equivalent of ions, and c_o the approximate concentration of H^+ ions in distilled water. The table provides just sufficient data to crudely estimate these parameters. Straightforward algebra yields

$$R_e \simeq 26.7 \; \Omega \qquad \text{(electrode area, A = 20.268 cm}^2\text{)}$$
$$R_s \simeq 5.34 \; \Omega$$
$$c_o \simeq 5.37 \times 10^{-5} \; \text{Neq.}$$

We thus might crudely estimate the specific junction resistance at about 541 Ω-cm^2 (R_e x A), as compared to the specific resistance of 1 cm^3 of a 1 N. solution, of 7.12 Ω-cm (R_s x tube area/tube length). For the test rig geometry, junction resistance and solution resistance would be equal for a concentration of about .2N.

Dynamic electrode characteristics: As indicated above, electrode properties are nonstationary on time scales measured in hours, minutes, or seconds. We shall define dynamic characteristics as those having time scales of 100 sec. or less. The data are consistent with the conjecture that reaction rates involve time scales longer than about .5 sec., that mass transport in solution has time scales on the order of .01-2 sec. (depending on concentration) and that charge relaxation times in solution are of the order of 10^{-5} sec.

The data of Experiment M generally show increase in impedance and

positive phase shift for very low and very high frequencies. This is
accounted for <u>qualitatively</u> by the circuit
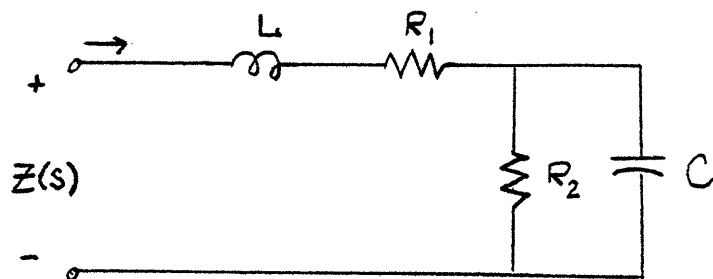
where L and R_1 are associated with the solution and R_2 and C are associated
with the electrode junctions. The former elements affect Z(s) at frequencies
over about 10^5 Hz, while the later elements affect Z(s) at frequencies below
about 100 Hz. This circuit is proposed merely as a mnemonic. If parameter
estimation were undertaken, all parameters would exhibit dependence on
frequency, concentration, temperature, amplitude of drive (Expt. N), junction
potential, etc., and would thus be of limited practical value. Furthermore,
the resulting circuit would be of questionable value in predicting transient
responses (as opposed to sinusoidal steady state). The difficulty in deter-
minining C ($\doteq$Cp) in Experiment C using a 1KHz signal is now apparent. Our
impedances appear less frequency-dependent than those measured by Schwann
and Geddes; this may be attributable to differences in electrode geometry,
plating procedure, ion species in solution, and other factors.

Future experiments will be concerned with the estimation of temperature
and pH effects, diffusion coefficients and reaction rates and types. While
many of the effects noted have been observed by others, our experiments at
least provide convincing demonstration that electrode properties are not so
simple as often supposed.

Appendix: Numerical Data for Lab Experiments

PLATING 4 min @ 0.6ma each electrode
ELECTROLYTE 0.05N   NaCl

Data for Figures B-1, B-2

Time (SEC)	Voltage (VOLTS)	Current (MA)	
0	+1.0	+06.0	
30	2.0	13.0	
35	2.0	4.5	
60	2.0	4.5	
90	2.0	4.5	
120	1.0	.82	
130	1.0	.6	
160	1.0	.5	
190	1.0	.42	
220	1.0	.4	
250	2.0	3.2	
280	2.0	3.1	
320	2.0	3.1	
350	3.0	9.8	gas evolves on cathode
380	3.0	9.8	gas
400	1.0	.7	
410	1.0	.9	
430	1.0	.7	
440	1.0	.6	
500	1.0	.4	
560	2.0	3.5	
570	2.0	3.3	
585	2.0	3.2	
620	2.0	3.1	
630	1.0	-00.5	
640	1.0	+00.4	
660	1.0	.4	
690	1.5	.8	
710	1.5	.7	
750	1.5	.63	
780	2.5	6.2	after 5 sec overshoot
805	2.5	6.2	
835	2.0	3.2	
885	2.0	3.16	
910	3.5	14.5	
930	3.5	14.5	

Time (SEC)	Voltage (VOLTS)	Current (MA)	
950	+0.5	-01.0	
965	.5	+00.3	
1000	.5	.3	
1030	2.5	6.4	after 2 sec overshoot
1045	2.5	6.25	
1080	2.5	6.22	
1140	1.5	.6	
1170	1.5	.6	
1230	1.5	.58	
1250	-1.5	-08.8	
1280	-1.5	-08.8	
1310	+0.5	+02.4	
1340	+0.5	+02.4	
1340	-0.5	-02.4	
1370	+1.0	+06.3	
1400	+1.0	+06.3	
1430	3.0	21.8	
1460	3.0	21.8	
1470	2.0	13.6	
1500	2.0	13.6	
1520	2.5	17.4	
1550	2.5	17.4	
off 15 min		00.0	
0	2.5	17.6	
10	2.5	7.0	
40	2.5	8.0	
90	2.5	8.0	anode noticeably darkened
120	-2.5	-17.6	
360	-2.5	-17.6	electrodes equally dark
360	+1.5	+09.8	
420	+1.5	+09.8	anode slightly darker
430	-1.5	-09.5	
460	-1.5	-09.5	
490	+2.5	+17.2	
550	+2.5	+17.2	
560	-2.5	-17.2	
590	-2.5	-17.2	electrodes equally dark

PLATING 4 min @ 0.6ma each electrode
ELECTROLYTE ~~DISTILLED~~ distilled water

C_p-equivalent parallel capacitance   D-dissipation factor

measured on 100uuf scale

C_p (muf)	D	Data for Figure C-1
.084	17
.077	19.5
.125	12
.123	12.3
.036	40
.049	30
.096	16
.158	9.5
.22	7
.059	29
.038	40
.033	45
.031	47
.030	49
.28	5.6

measured on 1muf scale

.14	10.5
.065	24
.13	11.5

PLATING 4 min @ 0.6ma each electrode
ELECTROLYTE ~~QWQNNWNNWW~~ distilled water

Time (MIN SEC)	Voltage (VOLTS)	Current (MA)
X 0	37.50	.0
3	37.50	.373
5	37.50	.381
8	37.50	.389
9	37.50	.391
10	37.50	.392
11	37.64	.393
12	37.64	.395
13	37.64	.397
14	37.80	.398
15	37.80	.400
16	37.50	.399
17	37.50	.401
18	37.50	.402
19	37.50	.403
20	37.50	.404
21	37.50	.405
22	37.50	.406
23	37.50	.407
24	37.50	.408
25	37.05	.404
26	36.48	.398
27	37.85	.372
28	27.65	.329
29	25.75	.288
30	21.25	.243
31	17.05	.201
32	14.75	.177
33	13.55	.164
34	12.90	.140
35	12.90	.140
36	12.90	.140
37	12.90	.141
38	12.90	.141
39	12.90	.141

Data for Figures D-1, D-2

Time (MIN)	Voltage (VOLTS)	Current (MA)
40	12.90	.142
41	11.68	.129
42	9.43	.105
43	6.92	.079
44	4.06	.049
45	. 3.36	.042
46	2.85	.036
47	1.97	.027
48	.67	.014
49	.15	.008
50	-0.17	+.005

meter reads +.006ma
with no input

PLATING 4 min @ 0.6ma each electrode
ELECTROLYTE X̶X̶X̶X̶ 0.01N NaCl

Time (MIN)	Voltage (VOLTS)	Current (MA)	
	.001	.012	
	-.002	-.009	
	+.149	+.092	
	.149	.089	
0	.149	.090	
1	.149	.089	
2	.149	.088	
3	.149	.087	
4	.149	.087	
5	.258	.161	
6	.347	.222	
7	.568	.374	voltage wildly fluctuating ±.01
8	.869	.581	" "
9	.85	.574	" "
10	.856	.568	current dropping
11	.856	.565	
12	.852	.562	
13	.851	.556	
14	.849	.552	
15	.847	.548	
16	.846	.543	
17	1.098	.711	
18	1.090	.684	
18	1.440	.909	
19	1.4045	.843	
20	1.405	.772	
21	1.405	.736	
22	1.4045	.680	
23	1.4045	.561	
24	1.4045	.510	
25	1.4045	.490	
26	1.4045	.476	
27	1.4045	.461	
28	1.4045	.460	wire knocked loose and replaced
29	1.4045	.449	

Time (MIN)	Voltage (VOLTS)	Current (MA)
30	1.4045	.445
31	"	.440
32	"	.435
33	"	.432
34		.431
35		.429
36		.423
37		.418
38		.411
***** 38.5		.410
39		.411
40		.415
41		.426
42		.438
43		.443
44		.445
45		.446
46		.448
47		.445
48		.441
49		.438
50		.436
51		.439
52		.440
53		.439
54		.436
55	1.405	.433
56	1.405	.430
57	1.405	.429
58	1.4055	.427
59	1.406	.423

Time (MIN)	Voltage (VOLTS)	Current (MA)

Time (MIN)	Voltage (VOLTS)	Current (MA)
60	1.406	.420
61	1.4065	.417
62	1.407	.415
63	1.407	.412
64	1.4075	.409
65	1.408	.406
66	1.408	.408
67	1.408	.414
68	1.407	.419
******68.5	1.407	.420
69	1.407	.419
70	1.407	.417
71	1.407	.413
72	1.4075	.408
73	1.408	.403
******73.5	1.408	.402
74	1.4085	.403
75	1.4085	.405
******75.5	1.4085	.406
76	1.4085	.405
77	1.4085	.404
78	1.4085	.402
79	1.4085	.401
80	1.4085	.405
******80.5	1.4085	.406
81	1.4085	.405
82	1.4085	.403
******82.5	1.4085	.402
83	1.4085	.404
84	1.4085	.407
85	1.4080	.415
86	1.4065	.427
87	1.4060	.431

Data for Figure E-2

(MIN)	(VOLTS)	(MA)	(MIN)	(VOLTS)	(MA)
0	1.38	.0	36	1.429	.213
1	1.38	.0	37	1.429	.214
2	1.38	.0	38	1.429	.216
3	1.38	.560	39	1.429	.218
4	1.38	.440	40	1.429	.221
5	1.40	.373	41	rechecked zero of voltmeter	
6	"	.361	42	1.4285	.223
7	"	.347	**42.5	1.4285	.224
8		.333	43	1.4285	.221
9		.321	44	1.4285	.216
10		.310	45	1.429	.210
11		.303	46	1.429	.204
12		.293	47	1.4295	.199
13	1.405	.292	**47.5	1.4295	.198
14	1.413	.295	48	1.430	.199
15	1.414	.300	49	1.430	.202
16	1.4165	.302	50	1.430	.207
17	1.4165	.304	51	1.4295	.213
18	1.417	.299	52	1.4285	.222
19	1.4175	.293	53	1.428	.233
20	1.4175	.284	54	1.426	.245
21	1.418	.278	55	1.4245	.254
22	1.419	.274	56	1.4245	.261
23	1.420	.271	57	1.4235	.269
24	1.420	.268	58	1.4230	.275
25	1.420	.262	59	1.4230	.278
26	1.421	.253	60	1.4230	.279
27	1.422	.243	61	1.4230	.278
28	1.423	.232	62	1.4230	.273
29	1.425	.224	63	1.4230	.267
30	1.426	.216	64	1.4235	.265
31	1.427	.210	65	1.4245	.266
32	1.4275	.206	66	1.424	.275
**32.5	1.4275	.205	67	1.422	.297
33	1.4285	.208	68	1.420	.320
34	1.4285	.210	69	1.418	.330
35	1.4285	.212	**69.5	1.418	.334

(MIN)	(VOLTS)	(MA)	(MIN)	(VOLTS)	(MA)
70	1.4185	.320	99	1.431	.204
71	1.420	.303	100	1.431	.207
72	1.4215	.290	101	1.431	.205
73	1.4225	.279	102	"	.200
74	1.4235	.270	103		.197
75	1.424	.266	104		.194
76	1.4245	.263	105		.189
77	1.4245	.261	106	1.431	.183
78	1.4245	.259	107	1.4325	.176
79	1.425	.257	108	1.433	.171
80	1.425	.257	109	1.433	.165
81	1.425	.257	110	1.434	.161
82	1.425	.256	**110.5	1.4343	.160
83			111	1.4345	.161
84	1.4255	.247	112	1.4345	.164
85	1.4255	.248	113	1.4345	.167
86	1.426	.244	114	1.4345	.173
87	1.4265	.238	115	1.4335	.182
88	1.4265	.234	116	1.432	.192
89 Voltage measurement now taken across supply			117	1.4305	.206
			118	1.429	.221
89	1.451	.232	119	1.4275	.241
90	1.451	.227	120	1.426	.251
**90.5	1.451	.225	121	1.426	.250
91	1.451	.228	122		
92	1.451	.235	123	1.426	.248
93	1.451	.242	124	1.426	.243
**93.5	1.451	.244	**124.5	1.426	.242
94	1.451	.237	125	1.426	.245
95	1.451	.224	126	1.426	.251
Voltage measurement back across cell. In addition sensor lead connected across cell			127	1.4255	.255
			128	1.4255	.248
			129	1.426	.233
			130	1.428	.219
			131	1.430	.208
96			132	1.4305	.200
97	1.431	.203	133	1.431	.194
98	1.431	.202	134	1.4315	.191

(MIN)	(VOLTS)	(MA)	(MIN)	(VOLTS)	(MA)
135	1.4315	.188	167	.6525	.127
136	1.4315	.184	168	.6525	.127
137	1.432	.182	169	.6525	.127
138	1.4325	.183	170	.6525	.128
139	1.432	.186	**170.5		.166
140	1.432	.189	170.75	.732	
141	1.4315	.189	171	.732	.142
142	1.432	.185	171.25	.7325	.139
143	1.432	.180	171.5		.138
144	1.4325	.175	171.75	.7325	.137
145	1.433	.172	172	.733	.136
146	1.4335	.170	173	.733	.132
147	1.4335	.169	174	.7335	.128
148	1.4335	.170	175	.734	.125
149	1.4335	.171	176	.734	.123
150	1.4335	.171	177	.734	.122
151	1.4335	.169	178	.734	.123
152	1.4335	.165	179	.734	.124
153	1.434	.162	180	.734	.127
*153.5	.67	-.034	181	.734	.129
153.75		.026	182	.7335	.130
154	.658	.080	183	.7335	.131
154.5		.099	184	.7335	.130
154.75	.654		185	.7335	.128
155	.654	.112	186	.7335	.125
155.5	.653	.118	187	.7335	.121
156	.653	.122	188	.7340	.117
157	.653	.127	189	.734	.113
158	.6525	.131	190	.735	.110
159	.6525	.133	191	.7355	.108
160	.6525	.133	192	.7355	.108
161	.6525	.132	193	.7355	.109
162	.6525	.130	194	.7355	.111
163	.6525	.129	195	.7355	.114
164	.6525	.127	195.25		.583
165	.6525	.127	195.5	1.73	.399
166	.6525	.127	196	1.763	.322
			196.5	1.7665	.301

(MIN)	(VOLTS)	(MA)	(MIN)	(VOLTS)	(MA)
197	1.767	.296	228	-0.101	-0.066
198	1.767	.293	228.5	-0.053	-0.032
199	1.767	.292	229	-0.040	-0.022
200	1.767	.292	229.5	-0.019	-0.008
201	1.767	.292	230	-0.012	-0.003
202	1.767	.293	230.5	-0.0045	-0.000
203	1.767	.293	231	+0.0009	+0.008
204	1.767	.292	231.5	0.00365	0.027
Switch leads			232	0.112	0.080
204.75		-1.642	233	0.1455	0.102
205		-1.252	234		
205.5	-1.671		235	-2.787	-2.12
205.75		-1.253	236	-2.787	-2.12
206	-1.671	-1.253	236.5	-4.1665	-3.18
207	-1.671	-1.253	237	-5.207	-3.98
208	-1.671	-1.253	237.5	-6.8425	-5.83
209	-1.671	-1.254	238	-8.482	-6.45
210	-1.6715	-1.255	238.5	-10.425	-7.92
211	-1.6715	-1.256	239	-10.425	-7.84
212	-1.671	-1.257	240	-10.425	-7.77
213	-1.6705	-1.257	241	-12.59	-9.29
214	-1.6705	-1.258	241.5	-12.59	-9.24
215	"	"	242	-12.59	-9.21
216	"	"	242.5	-15.44	-11.26
217	"	"	243	-15.44	-11.20
218	"	"	243.5	-24.44	-17.8
219	"	"	244	-33.98	-24.9
220	-1.54	-1.158	244.5	-40.38	-20.5 gas
221	-1.540	-1.158	245	-40.38	-20.0
222	-1.540	-1.158	246	-40.38	-28.6
223	-0.400	-0.290			
224	-0.400	-0.290			
225	-0.161	-0.111			
226	-0.162	-0.112			
*226.5	-0.121	-0.081			
227	-0.121	-0.081			
227.5	-0.101	-0.066			

Data for Figure E-3

(HR-MIN)	(VOLTS)	(uA)
1522:30	1.4310	771
1523	1.4330	766
1523:30	1.4345	763
1524	1.4355	760
1524:30	1.4365	757
1525		755
1525:30	1.4370	753
1526	1.4380	752
1526:30	1.4380	752
1527	1.4380	752
1527:30	1.4376	753
1528	1.4368	755
1528:30	1.4363	757
1529	1.4354	758
1529:30		
1530	1.4348	761
1531	1.4338	764
1532	1.4329	767
1533	1.4318	769
1534	1.4288	778
1535	1.4274	783
1536	1.4264	785
1537	1.4235	792
1538	1.4207	798
1539	1.4200	800
1540	1.4194	802
1541	1.4184	805
1542	1.4190	803
1543	1.4216	797
1544	1.4235	792
1545	1.4213	797
1546	1.4192	804
1547	1.4180	807
1548	1.4169	810

Anode now yellow.
Cathode darker brown.

(HR-MIN)	(VOLTS)	(uA)
Switch supply polarity		
1552	1.0415	871
1553	1.0355	872
1554	1.0355	873
Reverse cell connections.		
Reverse sensing leads.		
1558	1.0590	869
Switch supply polarity		
1600	1.3045	-003
Reverse sensing leads.		
1600:30	1.0900	-870
1614	Gas on anode.	

Original hook-up with 100 ohm
resister in place of cell
measured a constant 23.50 mv
across resistor with a current
of 228 uA changing to 227 uA
over a period of 45 minutes.

Data for Figure F-1

(HR-MIN)	(VOLTS)	(mA)	
1641	.068	1.00	
	.135	1.93	
	.200	2.86	
	.265	3.79	
	.460	6.60	
	.594	8.47	
	1.188	17.2	
	1.608	23.5	
	2.700	39.7	
	3.628	53.5	
	4.559	67.3	
	5.489	81.1	Gas on anode.
	6.425	91.1	
	6.425	70.0	Ammeter scale change.
	7.610	85.0	Gas streaming from anode.
	8.586	98.0	
	9.555	111.	Anode almost bare.
	10.57	125	
	11.11	132	
	16.14	201	
	20.52	258	
	22.92	286	
	25.82	318	White film on top half of cathode.
1703	32.6	405	Gas coming from three points on cathode. No film in three lines
	39.84	510	where gas rises across cathode.

Gas accumulates at bottom of cathode. White disappears at zero current.

	(VOLTS)	(mA)
	2.93	17.2
	6.72	61.2
	9.57	92.6
	16.0	165.
	21.0	224
	27.5	304
	32.6	367
	39.1	451
	41.0	473
0sec	-41.1	-620
15sec	-41.1	-550
25sec	-41.1	-568
35sec	-41.1	-583
45sec	-41.1	-597
70sec	-41.1	-612

OPEN CIRCUIT CELL VOLTAGE

Time (SEC)		(mV)
0		43
1-20		0
200		34
200-220		0
225	5	7
230	10	10
	15	12
	20	14
	25	15
	30	16
	45	18
	60	19
	75	21
	87	22
	100	23
	115	24
	131	25
	152	26
	171	27
	195	28
	222	29
	251	30
	285	31
	325	32
	369	33
	422	34
	497	35
	585	36
	662	37
	779	38
	1139	38
1140-1160		0
1165	5	8
	10	11
	15	13
	20	14
	25	15
	30	16

Time (SEC)	(mV)
35	17
40	18
45	18
50	19
54	20
57	21
67	22
79	23
93	24
107	25
122	26
140	27
160	28
192	29
215	30

Data for Figure H-1

(MIN)	(mV)	(muA)	
0	0.46	146	
	1.25	117	
	1.46	190	
	1.87	210	
2	2.20	210	
	2.39	210	
	2.77	210	μA Switch polarity-goes off scale. Switch back
	0.00	.3⁻	1mV transient
	0.00	.280	
	0.08	.314	
	1.08	.260	
	2.27	.222	
	2.60	.258	
	3.70	.216	
	3.49	.220	
	3.53	.194	
	5.26	.220	
	4.41	.262	
	3.87	.244	
	2.11	.340	
	1.46	.370	
	0.94	.310	
	-0.00	-.346	
	-1.70	-.396	
	-2.48	-.408	
25	-3.04	-.404	
	-4.27	-.456	
	-3.05	-.290	
	-2.60	-.327	
	-1.72	-.281	
	-1.16	-.274	
	-0.77	-.263	
0sec	-0.26	-.240	Current starts oscillating.
	"	-.320	
	"	-.260	
	"	-.320	
	"	-.280	
	"	-.310	
30sec	"	-.295	
	"	-.305	
	"	-.298	
	+0.45	+.200	

(SEC)	(mV)	(uA)	
	2.4	.465	
	7.0	.500	
	13.0	2.4	
	25.5	6.3	
	48.4	16.5	
	57.2	28.0	
	65.0	38.0	
	75.3	53.0	
	89.0	72.5	
0	101.0	90.	
10	115.3	90.	
20	418.	90.	Voltage still rising. Reverse leads.
30	-135.	-2.0	
40	-97	-1.9	
50	-80		
60	-75		
80	-61	-1.8	
100	-51		
120	-47	-1.6	
140	-41		
160	-35	-1.6	
180	-20	-1.55	

Data: Exp. I

TIME	Voltage(mV)	Current(uA)	Time	Voltage(mV)	Current(uA)
1430	-0.9	.390	1506	-82.0	.700
	-0.3	.421		-102.0	.890 transient
	-0.4	.410		-110.5	.800 "
	-0.1	.419		-115.0	.760 "
	-1.3	.337	1509	-118.0	.722 "
	-0.3	.420	1510:30	-121.5	.700 "
	-3.5	.258	1511:15	-123.5	.680 "
	-5.2	.180		change voltage	
	-7.0	.100	1512:30	-137.0	.740 transient
	-9.8	.026	1513:30	-141.0	.710 "
	-15.0	-.112	1514	-142.0	.695 "
	-21.0	-.234		change voltage	
1438	-32.5	-.330		-154.2	.780 transient
	-48.6	-.460		-165.0	.860 "
	-61.3	-.620	1515	-166.1	.840 "
	-73.6	-.680	1517:30	-185.6	.925 "
	-10 change polarity		1518:30	-197.9	1.000 "
	-11.3	-.222	1519	-201.4	.972 "
	+11.4	-.950	1519:30	-203.3	.950 "
	8.3	-.620	1520	-204.6	.940 "
	4.2	-.380	1520:30	-205.7	.930 "
	3.3	-.480	1521:30	-207.8	.910 "
1453	1.7	-.400	1522	-208.6	.902 "
	1.6	-.440		change voltage	
	1.1	-.437	1523	-181.6	.690
	0.7	-.390	1524	-151.5	.505
	0.1	-.407	1525:30	-103.4	.200
	-0.7	-.393		-56.1	.100
	-0.1	-.410		-35.3	-.280
	+2.0	-.482	1532	-19.0	-.600
	1.0	-.400		-6.5	-.930
	-3.4	-.157		0.0	-1.250
	-9.0	-.020		+6.0	-1.180
	-10.7	.000		change polarity	
	-13.5	+.030	1535	-43.5	($\frac{?}{}$).760
	-17.0	.180		-35.4	+.070
1504	-23.5	.310		-11.8	.660
				+5.5	1.100
				17.3	1.380

TIME	Voltage(mV)	Current(uA)	Time	Voltage(mV)	Current(uA)
1543:30	26.5	1.830	1606	-35.5	43.0
	39.1	2.550	1606:30	-44.7	62.0
	48.4	3.550	1609	-62.4	81.3 transient
	53.4	4.600	1609:30	-70(approx)	110.0 transient
	54.2	6.270	1610	-390	transient
1548:30	58.3	13.0	1610:30	-402	108 transient
1550	63.2	22.6 transient		change voltage	
1550:30	60.8	22.8 "	1614	-87.3	.17
1551	59.1	22.8 "	1616	-61.9	-.05
1551:30	57.9	22.7 "	1618	-33.4	-.55
1552	57.0	22.8 "	1618:30	-15.6	-1.3
1552:30	56.4	22.8 "	1620	-5.8	-1.5
1553	55.9	22.8 "		change polarity	
1553:30	55.5	22.8 "	1621	-33	-1.1
1554	55.1	22.8 "	1622	-48.3	-1.0
1554:30	54.8	22.8 "	1623	-31.5	-.35
1555	54.5	22.8 "	1624:30	+19.0	+3.9
	change voltage		1625:30	23.9	8.5
	64.6	43.0	1626:30	29.2	15.0
	68.7	62.0	1627	36.1	27.5
1556	72.0	81.0		45.4	48.5
	75.0	103.0	1628	53.9	67.7
	62.7	60.5	1629	62.9	110
	54.9	42.2	1629:30	64.8	112
	43.4	23.0	1630	67.0	111
1600	18.6	3.7		14.2	4.2
	9.2	.025		change polarity	
	3.6	1.32		1.7	4.4
	2.7	1.45		-2.5	4.33
	change polarity		1632	-31.9	43
	10.6	1.30		-41.1	70.5
	6.6	.12		-49.0	100.0
	-2.7	3.0			
	-9.5	5.8			
	-20.7	13.3			
	-27.8	23.0			

Bare   .01N

Time(MIN)	Voltage(mV)	Current
0	3.2	less than 1muA increasing
1	3.4	"
2	3.6	"
3	3.8	
4	3.9	
5	4.0	
6	4.1	
7	4.2	
8	4.3	
9	4.4	
10	4.45	
11	4.4	less o
12	4.5	"
13	4.55	"
14	4.55	curr
15	4.45	chan
16	4.45	less than .2muA
17	4.45	
18	4.40	
19	4.35	
20	4.25	
21	4.00	
22	3.9	less than .4muA
23	3.75	
24	3.6	
25	3.5	
26	3.45	current increasing
27	3.45	
28	3.5	

current always less than 1muA

29	3.5	less .4muA incr
30	3.5	"
31	3.55	"
32	3.65	"
33	3.8	"

~4.5 mv

~3.2 mv

28 min

less
" min
"

curr
chan

QRB 30-1

1.2K   1M

HP425A

WAVETEK
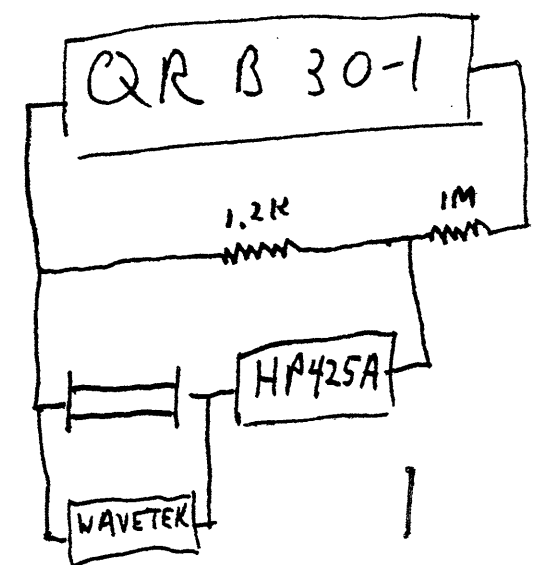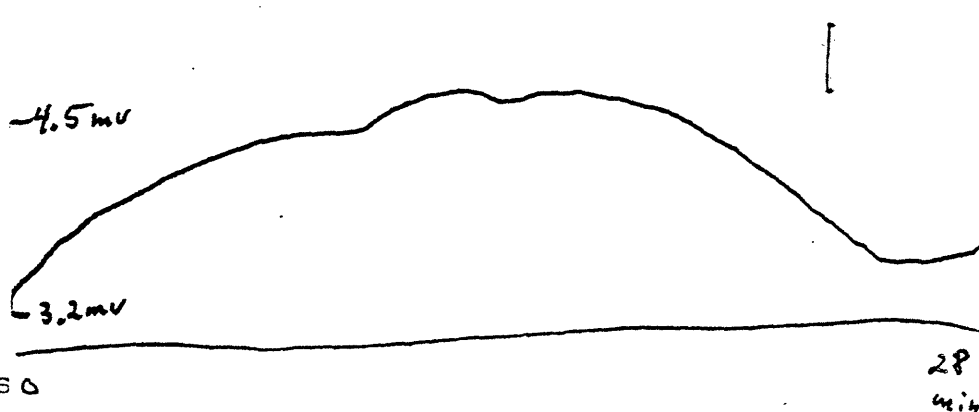
Time(MIN)	Voltage(mV)	Current
34	3.9	
35	3.95	
36	4.0	
37	4.05	decreasing
38	4.0	
39	4.0	
40	3.95	
41	3.9	
42	3.8	
43	3.8	
44	3.75	
45	3.7	
46	3.6	
47	3.55	
48	3.5	
49	3.45	
*58	3.10	zero current
60	3.15	+.8muA
62	3.10	.4
64	3.15	.4
70	3.10	.4
74	3.0	1.8muA
75	2.9	2.0
75	2.9	2.6
77	2.80	3.0muA

(HR-MIN)	(mV)	(uA)	(HR-MIN)	(mV)	(uA)
1750:00	0.0	-5.3	1813:00	32.92	54.3
1	0.0	-2.8		33.77	55.8
4	0.0	-1.9		34.77	57.6
6	0.0	-1.7		35.73	58.8
7	0.0	-1.15		36.68	60.2
9	1.20	+0.15		37.65	62.0
1800:00	2.00	+1.55		38.63	63.8
	2.55	2.50		39.71	65.7
	2.70	2.68	1814	40.72	67.0
1801	4.0	5.0	1815	37.66	62.0
	4.7	6.2		33.82	55.6
1802	6.45	9.1		30.87	50.1
	7.95	11.8		27.89	45.3
1803	8.9	13.3		25.00	40.2
	9.85	15.0	1817	21.93	35.5
	10.83	16.7		19.13	30.2
1805	11.9	18.6		14.64	21.9
	12.9	20.2	1818	10.83	15.5
	13.2	20.7		8.94	12.5
1806	13.64	21.2		7.00	9.5
	14.68	22.9		6.42	8.5
	15.62	24.5	1820	4.73	5.75
	16.45	25.9		3.00	3.00
	17.51	28.6		2.99	2.90
1807	18.45	29.0		2.20	1.80
	19.35	30.3		1.21	.0002
	20.95	34.2		.98	-.21
1808	21.94	36.1		0.00	-1.90
	22.89	38.0	Changed polarity of voltmeter.		
	22.92	38.6		-.80	-1.90
1809	23.84	38.8		+1.24	+0.52
	24.95	40.8	1830	+0.63	-0.40
1811	25.80	42.0		-0.67	-1.52
	26.77	43.9		-1.43	-2.55
	27.90	45.8		-2.79	-4.9
1812	28.97	47.7		-2.92	-5.0
	29.90	49.2	1833	-3.71	-6.23
	30.90	50.6		-4.57	-7.78
	32.00	52.5		-5.41	-9.10
	32.83	54.0	1834	-6.95	-12.10

(HR-MIN)	(mV)	(uA)	(HR-MIN)	(mV)	(uA)
	-7.87	-13.8		-0.45	+0.73
	-8.78	-15.1		-0.60	+0.30
	-9.73	-16.9		+1.25	+2.3
	-10.71	-18.6		+1.97	+3.2
	-11.71	-20.2		12.58	21.2
	-12.61	-21.8		22.75	50.3
	-12.68	-21.8		32.62	69.9
	-13.57	-23.0		42.27	88.0
	-14.51	-24.6		52.82	100.0
	-15.42	-26.0		62.75	117
1837	-16.47	-27.8		72.65	132
	-17.31	-29.3		82.64	151
	-18.96	-32.5		92.51	167
	-19.91	-34.4		102.4	185
	-20.95	-36.0	1858	112.35	202
	-21.90	-37.8		122.25	218
1839	-22.91	-39.0		132.40	234
	-23.90	-40.7		142.40	252
	-24.91	-42.2	1900	152.20	267
1841	-25.83	-43.9		162.10	283
1842	-26.89	-45.2		172.70	305
	-27.86	-46.9		182.67	325
	-28.80	-48.3		192.67	340
	-29.90	-50.0		202.60	360
	-30.65	-51.8		171.98	283
1843	-32.70	-54.8		142.20	235
	-34.64	-58.0		112.35	186
	-36.62	-61.4		82.60	137
	-38.57	-64.5		52.35	81.5
	-40.51	-67.9		22.90	32.5
1845	-37.70	-63.0	1907	3.05	-00.02
	-32.70	-54.1	Throw switch in circuit.		
	-27.91	-46.1	1908	-2.33	-7.0
	-22.99	-38.0		-12.43	-23.9
1847	-17.41	-27.0		-32.55	-64.0
	-12.60	-19.4		-62.70	-115.0
	-7.88	-11.6		-92.50	-163
1849	-3.87	-4.7			
	-1.81	-1.3			

(HR-MIN)	(mV)	(uA)	
1911	-122.35	-214	
	-152.25	-262	
	-182.65	-337	
	-202.60	-364	
	-152.70	-279	
	-152.15	-258	Ammeter scale change.
	-102.45	-173	
	-52.25	-84.3	
1918	-2.50	-0.65	Vmeter zero checked. Has perfect zero.

Slider resister added to circuit.

	(mV)	(uA)	
	+0.70	-0.013	
	-1.00	-1.95	
	-1.20	-2.10	
	-2.50	-4.40	
	-1.35	-2.40	
	-0.61	-1.15	
	0.00	+0.30	
	+1.00	+0.55	
	+0.57	-0.13	
	+0.75	+0.20	
	+1.35	-1.15	
	0.00	-1.35	Voltmeter zero problem.
	-0.75	-1.35	
	-0.92	-1.46	
	-1.62	-2.40	
	-1.90	-3.05	
	-0.31	-0.40	
	-0.00	-0.06	
	-0.13	-0.08	
	-0.26	-0.30	
	-0.47	-0.61	
	-0.50	-0.63	
	-0.70	-1.00	
	-0.71	-0.98	
	-0.96	-1.50	
	+1.20	+1.12	
	+1.06	+0.80	
	+0.62	+0.10	
	+0.45	-0.15	
	+0.33	-0.32	
	+0.05	-0.72	
	+0.00	-0.75	

Data for Figure L-1

(HR-MIN)	(mV)	(uA)	(HR-MIN)	(mV)	(uA)
	9.35	838.	1645	-92.19	-1115.
	7.57	670		-101.79	-1260
	6.83	620	Switch0sec	+101.79	+1400
	5.81	480	25sec	+101.79	+1300
	4.16	267	50sec	101.79	1280
	3.00	150	120sec	101.79	1260
	2.15	60.	180sec	101.79	1255
	1.73	47	1650	111.84	1370
	1.58	48		121.60	1485
	1.25	2.1		131.81	1525
1628	1.04	2.58		141.32	1750
	.83	.98		151.32	1890
	.64	-2.15		161.22	2000
	.58	-1.17		171.22	2130
	.45	-2.0		180.88	2275
	.00	-6.90		190.69	2405
Throw switch	.00	-4.20		200.64	2540
	-.34	-13.4	1654	190.64	2400
	-.52	-18.3		180.87	2280
	-1.32	-26.0		170.98	2130
	-2.90	-44.8		161.19	2005
	-3.90	-53.9		151.37	1895
	-4.83	-61.0		141.45	1760
	-5.79	-69.8		131.77	1625
	-6.79	-72.0		121.77	1500
	-7.59	-80.3		111.90	1390
	-8.53	-89.0		102.02	1250
1638	-9.53	-97.7		92.20	1120
	-10.14	-104.		82.34	1020
	-11.14	-112		71.93	828
	-12.06	-121		62.21	709
	-22.90	-247		52.44	593
	-32.25	-360		42.45	470
	-41.66	-470	Ammeter sticks	32.74	357
	-52.26	-597	1704	22.57	232
	-61.85	-704		12.92	199
	-71.78	-823	Ammeter sticks	8.33	66.0
	-81.36	-935		5.13	40

(HR-MIN)	(mV)	(uA)	(HR-MIN)	(mV)	(uA)
	4.38	25.7		-179.75	-2380
	3.08	13.1		-189.85	-2510
0sec	2.41	1.6		-199.44	-2620
10sec		1.8		-160.06	-2110
20sec		1.9		-110.90	-1460
30sec	1.87	2.0		-71.55	-920
50sec		2.05		-40.00	-480
70sec	1.87	2.20		-20.32	-230
100sec		2.36	1733	-10.28	-102
120sec		2.50	0sec	-1.20	+3.8
150sec	1.70	2.60	15sec	-0.83	+2.0
180sec		2.73	30sec	-0.80	+1.0
210sec	1.70	2.80	60sec	-0.65	+0.1
225sec		2.25	120sec	-0.52	-0.2
270	1.70	3.05	180sec	-0.32	-0.5
1715:00 Switch	.38	-47.8	240sec	-0.22	-0.55
1715:10	-1.22	-46.0	Throw switch		
	-2.06	-55.6	0sec	+0.03	+19.2
	-2.87	-64.3	30sec	+0.07	+18.4
	-3.74	-75.8	60sec	+0.07	+18.1
	-4.61	-85.8	Throw switch		
	-5.55	-96.0	0sec	-0.48	-7.8
1720	-9.12	-140	30sec	-0.48	-7.8
1721	-19.51	-270	1745 Throw switch		
	-29.83	-420	0sec	+0.13	+17.6
	-39.59	-544	30sec	+0.13	+17.6
	-49.59	-677	Throw switch		
	-59.28	-799	0sec	-0.48	-8.8
	-69.08	-919	30sec	-0.48	-8.8
	-79.70	-1080	Throw switch		
	-89.44	-1195	1747	+0.18	+17.6
	-99.14	-1310			
	-109.00	-1440			
	-119.66	-1585			
	-129.40	-1700			
	-139.57	-1825			
1727	-149.30	-1990			
	-159.14	-2100			
	-169.00	-2215			

Data: Exp. M1

Freq (Hz)	!Z! dual	!Z! x-y	/Z	/Z	/Z
.01	∞	18.5K	63	60	56.5
.03	16.43K	14.2K	57	60	76.5
.1	4.94K	5.41K	72	63	60.4
.3	3525	3080	57	51	73.5
1.	1370	1358	53	53	51.4
3.	682	733	24.2	53	49.9
10	453	462	23	21	20.3
30	432	403	10.4	10	11.65
100	389	395	4.0	3.5	4.86
300	386	386	1.7	0.0	0.0
1K	494	368	0.0	0.0	0.0

Other generator

10	562	483	19.9	20	18.7
30	504	427	9.2	9	9.3
100	494	405	4.0	5	2.15
300	429	406	1.4	0.0	0.0
1K	433	406	.6	0.0	-2.5?
3K	448	399	0.0	0.0	0.0
10K	457	399	.6	0.0	1.
30K	474	412	1.7	0.0	.4
100K	465	305	5.7	10.	(6.)
300K	504	222	18.7	53.	21.9

!Z! was calculated as !V!/!I! measured on both dual trace and x-y scopes.
/Z was measured directly on x-y scope.

V_{gen}, V_{cell}, V_R
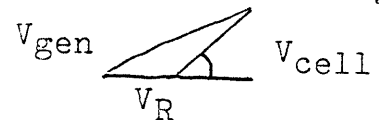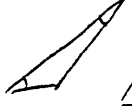
/Z was calculated from V_{cell}, V_R, and the angle between generator and Resistor.
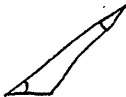
V_{cell}, V_R
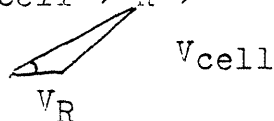
/Z was also calculated as sum of angles between generator and Resistor, and generator and cell.

Rare   .1N

Freq (Hz)	!Z! dual	!Z! x-y	/Z	/Z	/Z
10	140	147	40	48.8	
30	87.5	72.2	35.2	35.8	
100	63.6	63	19.5	21.1	
300	54.9	56	8	8.05	
1K	53.8	54.8	3	1.3	
3K	56	54.7	.6	0.0	
10K	56	54.7	.6	.67	
30K	56	55.4	2.5	2.9	
100K	56	48.1	6.9	2.9	

Bare   .1N

Freq (Hz)	!Z! dual	!Z! x-y	∠Z	∠Z

990 ohm resister

.01	483	507	3.5	-8
.03	454	433	5.5	5.75
.1	354	381	14.5	17
.3	283	313	27.7	36.5

68 ohm resister

.1	341	425	35.1	24
.3	238	353	40.5	46.2
1	176.3	178	41.2	55.2
3	1.4.5	105.6	32.6	35.05
10	74.9	75.3	17.8	17
30	64.8	68	7.3	9.7
100	61.8	65.7	2.3	1.15
300	61.8	65.2	1.45	-4
1K	64.8	65.2	0.0	-2

Other generator

10	84.9	82	24.2	25.3
30	70.9	60.7	11.2	12
100	75.5	64.8	4	5.1
300	61.8	64.9	1.4	4.68
1K	71.7	64.8	.57	0.0
3K	79.7	66.7	0.0	0.0
10K	84.9	63.8	0.0	0.75
30K	84.9	65.2	3.5	1.7
100K	84.9	66.8	8.85	7.9
300K	82.5	82.8	18.35	17.6

Chlorided .01N

Freq (Hz)	!Z! dual	!Z! x-y	/Z	/Z
.01	.685	.607	0.0	0.32
.03	685	643	0.0	0.0
.1	685	650	0.0	0.64
.3	685	575	0.0	0.0
1	605	597	0.0	0.0
3	685	606	0.0	0.0
10	623	592	0.0	0.0
30	623	595	0.0	0.0
100	643	601	0.0	0.0
300	623	588	0.0	0.0
1K	623	603	0.0	0.0
Other generator				
10	664	622	0.0	0.0
30	643	623	0.0	0.35
100	664	617	0.045	0.24
300	643	614	0.0	0.12
1K	643	610	0.0	0.0
3K	605	607	0.046	0.0
10K	605	604	0.92	0.43
30K	623	536	1.6	4.75
100K	623	530	6.6	10
300K	623	763	10.3	14.5

Chlorided .1N 106Ω $47°F$

Freq (Hz)	!Z! dual	!Z! x-y	$\angle Z$	$\angle Z$
.01	68.5	73.2	3.4	1.6
.03	68.5	64.3	2.05	1.25
.1	70.6	76.8	1.33	0.89
.3	73	76.2	1.06	1.35
1	70.6	77	0.57	1.13
3	70.6	74	0.54	0.88
10	70.6	72.2	0.85	0.9
30	68.3	72.2	1.1	1.34
100	68.3	71.2	0.59	1.15
300	66.2	73	0.55	1.1
1K	66.2	68.1	0.0	0.0

Other generator

10	70.6	69.4	0.0	0.0
30	66.2	70.6	0.0	0.0
100	64.3	69.6	0.0	0.21
300	64.3	70.4	0.54	0.21
1K	66.2	70.2	0.55	0.0
3K	73	69.2	0.0	0.0
10K	70.6	69.0	1.1	0.91
30K	62.3	70.0	2.7	3.54
100K	70.6	69.8	8.5	7.65
300K	66.2	72.4	16.8	17.2

Thermodynamic Model of the Silver-Silver

Chloride Electrode in Salt Solution

W. Kohn and T. L. Johnson

I. Introduction

In this preliminary note, we formulate a Thermodyanmic model of the electrode-solution-electrode system shown in Figure 1. Our approach here
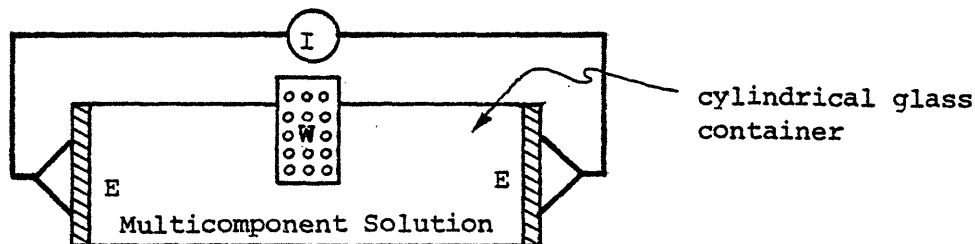
E : Disk electrodes

I : Passive recording instrument

W : Non diffusional wall variable length

Representative Scheme of the Electrode

Figure 1

is to present relations between mass and energy fluxes and the forces producing mass and energy transport throughout the system. The formulation relies heavily on a generalization of the Stefan-Maxwell equations (Fick's law) in the context of non-equilibrium thermodynamics [1]. Roughly, these equations establish linear relationships between the forces and the corresponding fluxes in the system.

The Stefan-Maxwell equations are field expressions of the local principles of mass, momentum and energy balances of the system [2]. And they fully characterize the electrochemical behavior of a multicomponent system under "small" distrubances provided that certain assumptions about the physical characteristics of the system components are satisfied. In the next section we establish these conservation relations for a general multicomponent medium, together with the respective assumptions about the characteristics of the

system that validate its use. In section III we discuss the validity of the equations for the system of fig. 1.

II. Multicomponent Equations of **Charge** in Terms of the Fluxes

The substantial conservation (balance) relations for multicomponent systems are introduced in [3], Chapter III. The discussion there is generally adequate for our purposes. They may be summarized as follows for a system of n components

(1) $\quad \dfrac{\partial c_i}{\partial t} = -(\vec{\nabla} \cdot \vec{N}_i) + R_i \qquad\qquad i = 1,2,3, \ldots n \quad \text{Continuity}$

(2) $\quad \dfrac{\partial}{\partial t} \rho\vec{v} = -[\vec{\nabla}\Psi] + \displaystyle\sum_{i=1}^{n} \rho_i \vec{g}_i \qquad\qquad \text{Motion}$

(3) $\quad \dfrac{\partial}{\partial t}\rho\,(U + \tfrac{1}{2}\,|\vec{v}|^2) = -(\vec{\Delta}\cdot\vec{e}) + \displaystyle\sum_{i=1}^{n}(\vec{N}_i M_i \cdot \vec{g}_i) \qquad \text{Energy}$

where c_i, ρ_i are the molar and mass concentrations of species i at each point in the system and at each time. The g_i are the body forces per unit mass acting on species i, $\hat{U}$ is the internal energy per unit mass, M_i is the molecular weight of species i, $\vec{v}$ is the mass average velocity

The variables $\vec{N}_i = c_i\vec{v}_i$, Ψ and e are the total fluxes of species i (in moles), momentum and energy, respectively, relative to any (arbitrarily chosen) fixed coordinates. The remaining terms are:

R_i = rate of formation of i in moles per unit volume and time by chemical reaction

$\displaystyle\sum_{i=1}^{n} \rho_i \vec{g}_i$ = volumetric rate of momentum increase resulting from body forces $\vec{g}_i$ per unit mass of each species

$\displaystyle\sum_{i=1}^{n} \vec{N}_i M_i \cdot \vec{g}_i$ = rate at which work is done on the system per unit volume by virtue of the body forces.

Any one of the n species continuity equations may be replaced by their sum, the equation of continuity of the system.

Each of the fluxes may be written as the sum of a <u>convective</u> flux, resulting from the motion of the fluid, and a <u>diffusion</u> flux relative to this motion, thus

(4) $\vec{N}_i = c_i \vec{v} + \vec{J}_i$ $i = 1,\ldots,n$

(5) $\vec{\Psi} = \rho \vec{v} \times \vec{v} + \vec{\pi}$

(6) $\vec{e} = \rho \left(\hat{U} + \frac{1}{2} \vec{v} \cdot \vec{v} \right) \vec{v} + \pi \cdot \vec{v}$

The significance of the diffusive J_i (mass flows), π (momentum flows) and $\pi \cdot \vec{v}$ (energy flows), will become apparent later, when we discuss their relation with their corresponding diffusion forces.

In order to find equations relating fluxes and forces that represent the mechanisms of mass transport at a local level, for this purpose, the effective framework is the theory of nonequilibrium thermodynamics, (local version) developed by Lars Onsager [4]. We briefly discuss some of its aspects, in particular the ones that make the use of the generalized Stefan-Maxwell equations plausible for describing our system. For a very comprehensive and complete review of this theory, reference [5] is recommended.

Diffusion and convective transport, like most spontaneous processes, are irreversible. In all such phenomena there is a tendency towards randomization (i.e., to reach the thermodyanmic state of minimum internal engergy). This natural characteristic makes the probability of return of the system to an earlier state very small; and, for systems for very large number of molecules - like ours - this probability essentially is zero (moreover, in Quantum-Thermodynamic studies of these systems the reversible paths are excluded from the σ-fields adapted to the dynamic evolution of the system). The quantitative measure of the degree of "randomness" in a system is its entropy, and <u>all</u> natural (spontaneous)

processes are accompanied by an increase in entropy. It seems reasonable, therefore, that a <u>complete</u> description of entropy changes (in time) taking place in a system should also provide the means to determine all the spontaneous processes which are possible in that system. That is, entropy changes are, in principle, <u>sufficient information to identify the dynamic structure of the system.</u> Although non classic, in the author's opinion, this assumption is the fundamental starting point for nonequilibrium thermodynamics, and in particular, will play an important role in the analysis of our system.

As a first step in **this** development we need a general conservation equation for entropy similar to those stated earlier for mass, momentum and energy:

$$(7) \quad \rho \, \frac{DS}{Dt} = -\vec{\nabla} \cdot \vec{J} + \sigma$$

where

$\quad S$ = entropy per unit mass

$\quad \vec{J_s}$ = entropy flux relative to the mass - average velocity

$\quad \sigma$ = volumetric rate of entropy production

Equation (7) is just a definition for local entropy; our problem ahead is to find out expressions for the individual terms in it; most particularly, for the rate of entropy production, since as our assumption above suggests, this will allow us to find a description for the processes that characterize the system. Further, we want this description to be expressed in terms of <u>measurable quantities</u> such as voltage and current, and quantities that can be estimated, such as

concentration. Hence, we must relate entropy to these quantities. Towards this objective we start by considering a slightly restricted version of the first postulate of nonequilibrium thermodynamics [1].

Postulate 1.

"Departures from local equilibrium are sufficiently small that all thermodynamic state variables may be defined locally by the corresponding quantities at equilibrium."

This postulate has proven to be reliable in systems involving macroscopic transport of statistically uniform particles (small molecules in aqueous solution) and apparently holds for our system.

We now assume that postulate 1 holds for our system; then the second law of thermodynamics can be written as

$$(8) \quad T\rho \frac{DS}{Dt} = \rho \frac{DU}{Dt} + \rho P \frac{D\vec{V}}{Dt} - \sum_i \frac{\mu_i}{M_i} \rho \frac{Dw_i}{Dt}$$

where T is absolute temperature $\bar{v} = \frac{1}{\rho}$ is the specific volume; μ_i is the partial molal free energy (chemical potential), w_i is the mass fraction of species i in the system.

Using equations (4) and (6) in (1) and (3) and the expression (14)

for the total derivative of a field quantity, i.e.,

$$\frac{DA}{Dt} = \frac{\partial A}{\partial t} + \vec{v} \cdot \vec{\nabla} A,$$

in (8), we obtain

$$(9) \quad \rho \frac{DS}{Dt} = - \vec{\nabla} \cdot [\vec{q} - \vec{j}_i \mu_i / M_i]$$

$$- \frac{1}{T} \{\vec{q} \cdot \vec{\nabla} \ln T + \sum_{i=1}^{n} (\vec{j}_i \cdot [T\vec{\nabla} (\frac{\mu_i}{TM_i}) - \vec{g}_i]$$

$$+ (\vec{\tau} : \vec{\nabla} \times \vec{v}) + \sum_{i=1}^{n} \frac{\mu_i r_i}{M_i}$$

where

j_i = mass flux of species i relative to mass average velocity

τ = shear stress tensor

r_i = rate of formuation of species i with respect to its molecular weight.

We now define entropy flux as

(10) $$\vec{j}s = \frac{1}{T}\left(\vec{q} - \vec{j}_i \frac{\mu_i}{M_i}\right)$$

Then, from (9), (10) in (7) we obtain the following expression for the volumetric rate of entropy production, σ:

(11) $$-T\sigma = \left(\left[\vec{q} - \sum_{i=1}^{n} \frac{\bar{H}_i}{M_i} \vec{j}_i\right] \cdot \vec{\nabla}\ell n\, T + (\vec{\tau}:\vec{\nabla}x\vec{v}) \right.$$
$$\left. + \sum_{i=1}^{n} (\vec{j}_i \cdot \vec{\Lambda}_i) + \sum_{i=1}^{r} \mu_i r_i \right)$$

where

$\bar{H}i$ = mass-average entropy of species i and

(12) $$\vec{\Lambda}_i = \vec{\nabla}_{T,p} \frac{\mu_i}{M_i} + \frac{\bar{v}_i}{M_i} \vec{\nabla}p - \vec{g}_i$$

and

(13) $$\vec{\nabla}_{T,p}\mu_i = RT\vec{\nabla}(\ell n a_i)_{T,p}$$

where R is the international gas constant and

a_i = Thermodynamic activity of species i.

This choice for the volumetric rate of entropy production, (11), is a modified version of the one given by Gyamarti [6]. The particular form obtained, presents very convenient features for the analysis of electrode-solution systems such as ours, and as we shall see, permits a nice characterization of phase transition phemonena at the electrical double layer in the solution in

the region immediately adjacent to the electrode surface. We list three important properties that are satisfied by this definition.

a - The entropy production is zero at equilibrium.

b - The source term is invariant to transformations of the form

$$\frac{\partial}{\partial t}\rho\hat{s} = -\nabla\cdot[\rho\hat{s}\vec{v} + \frac{\vec{q}}{T} - \sum_{i=1} \vec{j}_i \frac{\mu_i}{T}] + \sigma$$

(Material form of the entropy equation)

c - For a closed system with exchange of heat with its surroundings the proper (reversible) inequality for the total entropy is obtained:

(14)
$$\frac{ds_{tot}}{dt} = \int \frac{\partial}{\partial t}(\rho\hat{s})dv$$

$$= \int_{Atot} \frac{1}{T}(\vec{q}\cdot\vec{n})dA + \int_{v_{tot}} \sigma dv \geq$$

$$\int_{Atot} \frac{1}{T}(\vec{q}\cdot\vec{n})dA$$

The use in (13) of the chemical gradient rather than the total electrochemical-potential gradient is convenient for our system because it allows us to study the electrical potential, which is the main thermodynamic state that is directly measurable, by its affects in the solution as a body force acting on each species and consequently, as a driving term. Notice that this is just a notational and operational convenience rather than a major conceptual change.

A more convenient expression for the chemical gradient (e.g. (10)) is given by considering the coefficients of "influence" of all the species present in the system, and the mole fraction interaction of them with species i; that is,

$$(15) \quad \nabla_{T,p}\mu_i = \sum_{j=i}^{n} \left(\frac{\partial\mu_i}{\partial x_j}\right)_{T,p,x_k} \vec{\nabla}x_j$$

where

x_j = mole fraction of species j.

This is possible since we have assumed the validity of postulate 1.

We note that equation (11) is "complete" in the sense that it contains all the terms contributing to entropy production and that each term is the product of a flux and a "driving force."

It follows, from our discussion so far, that the entropy production rate should depend only upon the forces, fluxes and the physico-chemical nature of the system. This means that for any thermodynamic state the fluxes should depend only (locally) on the driving forces.

We want to determine these dependencies and this cannot be done based on the thermodynamic argument used up to this point. Before examining this point, it is worthwhile to note that the mass fluxes with respect to the mass average velocity sum to zero

$$(16) \quad \sum_{L=1}^{n} \vec{j}_i = 0$$

This implies, that equation (11) will be satisfied if we add an arbitrary function to each Λ_i. It will be specially convenient for the analysis of our system to replace the Λi by an augmented Λi^* of the form;

$$(17) \qquad \vec{\Lambda}_i^* = \vec{\Lambda}_i - \frac{1}{\rho} \vec{\nabla} p + \sum_{j=1}^{n} w_j \vec{g}_j$$

where the added quantity is the total force per unit mass acting on the fluid.

Then we have

$$(18) \qquad \sum_{L=1}^{n} (\vec{j}_i \cdot \vec{\Lambda}_i^*) = \sum_{L=1}^{n} \vec{j}_i \cdot [\vec{\Lambda}_i - \frac{1}{p} \vec{\nabla} p + \sum_{k=1}^{n} w_k \vec{g}_k]$$

The mass fluxes $\vec{j}_i$, can be expressed in terms of the respective species velocities as,

$$(19) \qquad \vec{j}_i = \rho_i (\overline{v}_i - \overline{v})$$

Thus, using (12) and (19) in (18) we obtain

$$(20) \qquad \sum_{i=1}^{n} \vec{j}_i \cdot \vec{\Lambda}_i^* = cRT \sum_{L=1}^{n} ([\vec{v}_i - \vec{v}] \cdot \vec{d}_i)$$

where

$$(21) \qquad cRT\vec{d}_i = c_i \vec{\nabla}_{T,p} \mu_i + (c_i \overline{v}_i - w_i) \vec{\nabla} p - \rho_i (\vec{g}_i - \sum_{k=1}^{n} w_k \vec{g}_k)$$

and

c = total molar concentration

c_i = molar concentration of species i

In (21) we have chosen to associate the density ρ_i with the "driving force" rather than with the "flux"; as we shall see this is very convenient for our purposes.

The quantity $CRTd_i$ has a very important physical significance as the **force per unit volume of solution tending to move species i relative to the solution.**

                        The total force per unit volume relative to the solution is zero. (Provided that the solution is not itself in turbulent hydraulic flow; certainly a condition that is satisfied in our case.)

$$(22) \qquad \sum_{L=1}^{n} \vec{d}_i = 0$$

Equation (22) is valid for non isothermal-non isobaric reacting mixtures [6] and thus provides a very useful check for determining whether all the "important" forces driving the system have been considered. We will have opportunity of using (22) in checking the validity of some simplifying assumptions in our model.

Now to determine the flux-force dependence, we require the second postulate.

Postulate 2.

"The fluxes are linearly and homogeneously related to the driving forces," i.e.;

$$(23) \qquad \vec{j}_i = \sum_{k} \beta_{ik} \vec{x}_k$$

where $\vec{j}_i$ = any flux appearing in the expression for σ (11). That is mass momentum , or energy.

$\vec{x}_i$ = any corresponding driving force, and the β_{ik}'s are "phenomenological coefficients" or transport properties (i.e, diffusion coefficients permittivity, etc.).

The flux force relations must be homogeneous because at equilibrium there must be no entropy production. They are not necessarily linear and the above equation (23) must be considered as a limiting case. Also, as we shall see, even for small gradients, in our system, the β_{ik}'s are functions of the driving forces and even, in some cases, of the flows as well.

Fortunately, one does not have to consider all the interrelations indicated by equation (23). It can be shown on the basis of symmetry [7], that coupling can occur only between driving forces and fluxes of the same tensorial order or between those varying in rank by even multiples.

One final simplification is made possible by the third postulate which simply states:

Postulate 3.

The β_{ij} are symmetric : $\beta_{ij} = \beta_{ji}$

The postulate was derived by Onsager on the basis of statistical mechanical arguments [4], and is supported by a huge amount of experimental data. We mention the fact that postulate 3 is <u>not</u> valid for processes involving subprocesses with entropy-reduction characteristics, i.e., biosynthesis. In our system these processes are not present.

Next we use the 3 postulates discussed above, and equation (21) to get relationships between body forces and fluxes in a system with chemical reactions among its elements.

The body force g_i acting on species i due to an electrostatic potential gradient $\nabla\phi$ is given by

$$(24) \qquad \bar{g}_{ie} = - \frac{\nu_i F}{M_i} \vec{\nabla}\phi$$

where, νi is the valence of species i in the solution, F is the Faraday constant and ϕ is the electrostatic potential. Thus, from (24) in (21) assuming that the force component due to pressure gradients is negligible we obtain,

$$(25) \qquad cRT\vec{d}_i = c_i\vec{\nabla}_T\mu_i + \left[\rho_i \frac{\nu i}{M_i} - \rho_i \sum_{k=1}^{n} w_k \frac{\nu_k}{M_k} \right] F \vec{\nabla}\phi \qquad i=1,\ldots,n$$

since

$$(26) \qquad \rho_i = c_i M_i$$
$$w_i = \frac{M_i}{m}$$

(25) can be written as,

$$(27) \qquad cRT\vec{d}_i = c_i\vec{\nabla}_T\mu_i + (c_i\nu_i - w_i\sum c_k\nu_k) F \vec{\nabla}\phi$$
$$i=1,\ldots,n$$

From (13) in (27) we obtain

$$(28) \qquad cRT\vec{d}_i = c_i RT\vec{\nabla}_T(\ell na_i) + (c_i\nu_i - w_i \sum_{k=1}^{n} c_k\nu_k) F\vec{\nabla}\phi \qquad i=1,\ldots,n$$

Since $a_i = \gamma_i c_i$, where γ_i is the chemical activity coefficient distribution of species i, equation (28) becomes

$$(29) \quad C R T \vec{d}_i = c_i R T \vec{\nabla}(\ln \gamma_i c_i) + (c_i \nu_i - w_i \sum_{k=1}^{n} c_k \nu_k) F \vec{\nabla}\phi$$

Using equation (29) in (20), we obtain

$$(30) \quad \vec{j}_i \cdot \vec{\Lambda}_i^* = [\vec{v}_i - \vec{v}] \cdot [R T c_i \overline{\nabla} \ln \gamma_i c_i + (c_i \nu_i - w_i \sum_{k=1}^{n} c_k \nu_k) F \nabla\phi]$$

Using (30) and (19) in (12) and (11); and the result in (1) we obtain,

$$(31) \quad \frac{\partial c_i}{\partial t} = -\overline{\nabla} \cdot [D_i R T C_i \vec{\nabla} \ln \gamma_i c_i + (c_i \nu_i - w_i \sum_{k=1}^{n} c_k \nu_k) F \overline{\nabla}\phi] + R_i \qquad i=1,\ldots,n$$

Equation (31) gives the dynamic behavior of the concentration distributions of each species in the solution. Recall that in this expression isothermal isobaric conditions were assumed. Notice also, that no charge neutrality was assumed. Our next task ahead is to obtain expressions for R_i, the rate of formation of species i due to chemical reaction. Before this, we complete

the formulation of the solution model by giving equations for the dynamics of the electric potential [ ]. These dynamics are given by two equations:

$$(32) \quad \vec{\nabla} \cdot (\varepsilon \vec{\nabla}\phi) = - F \sum_{j=1}^{n} \nu_j c_j \qquad \text{(Poisson equation)}$$

where ε is the electric permittivity of the solution,

$$(33) \quad \vec{J}(t) - \sum_{j=1}^{n} \vec{J}_j + \frac{\partial}{\partial t} \varepsilon \vec{\nabla}\phi = 0 \qquad \text{(Gauss law)}$$

where $\vec{J}(t)$ is the boundary-driving current density and $\vec{J}_j$ is the <u>ionic</u> current density of species j. That is $\vec{J}_j = 0$ if $\nu_j = 0$.

The current density distribution of species i is related to the mass flow $\vec{j}_i$ by the expression

$$(34) \quad \vec{J}_i = \nu_i F \vec{j}_i \qquad i=1,\ldots,n$$

From (16) and (34) we have

$$(35) \quad \sum_{i=1}^{n} \vec{j}_i = 0 \qquad \text{(Macroscopic electroneutrality)}$$

Thus (33) becomes

$$(36) \quad \vec{J}(t) + \frac{\partial}{\partial t} \varepsilon \vec{\nabla}\phi = 0 \qquad \text{(at the boundary)}$$

Equations (31), (32) and (36) constitute the representation of the model. Now, we proceed to determine expressions for the rate of production R_i.

The rate of production (or disappearance), of species j is given
by the following equation [ ].

$$(37) \qquad R_j = \sum_{i=1}^{p} \alpha_{ij} \sigma_i - c_j \frac{d\ln V}{dt}$$

where p is the number of <u>simultaneous reactions</u> occuring in the system, and
σ_i is the reaction rate of the i<u>th</u> reaction and V is the volume of reaction.
The σ_i's are obtained by a balance argument as in [1]:

$$(38) \qquad \sigma_i = s_i \prod_{j=1}^{\ell} c_i^{\beta_{ij}} - s_{-i} \prod_{j=\ell+1}^{n} c_i^{\gamma_{ij}} \qquad i=1,\ldots,p$$

where the coefficients β_{ji} and γ_{ji} are phenomenological coefficients termed
<u>degrees of cooperativity</u> of the ith reactant (or product, respectively) in
the jth reaction. For systems with non-organic univalent solutes and weak
equilibruim concentrations (as in the present case), these coefficients tend
to unity. We will assume

$$(39) \qquad \beta_{ji} = \begin{cases} 1 & \text{if the ith species is a reactant in the jth reaction} \\ 0 & \text{other wise} \end{cases}$$

$$j = 1,\ldots p \qquad i = 1,\ldots n$$

and

$$(40) \qquad \gamma_{ji} = \begin{cases} 1 & \text{if the ith species is a product in the jth reaction} \\ 0 & \text{otherwise} \end{cases}$$

$$j = 1,\ldots,p \qquad i = 1,\ldots,n$$

For a more detailed discussion of degrees of cooperativity see Aris [ ] and Nikishima [ ].

Next we find expressions for the reaction rate coefficients s_i and s_{-i} of the ith reaction in terms of the variables of the system. These coefficients are called the forward and backwards reaction coefficients of the ith reaction.

For a system evolving at isothermal conditions and assuming that the reactions at the surface of the electrodes are evolving near the saturation point, s_i, and s_{-i} are given by

$$s_i = k_{io} \exp(-\Delta H_i/RT) \qquad\qquad i = 1 \ldots \rho$$

(41)

$$s_{-i} = k_{-io} \exp(-\Delta H_i/RT) \qquad\qquad i = 1, \ldots \rho$$

where ΔH_i is the difference in enthalpy between products and reactants in the ith reaction and k_{io} and k_{-io} are phenomenological coefficients that depend only on the condition of the system at saturation conditions i.e., $\sigma_i = 0$).

Thus, using (38) with $\sigma_i = 0$, and (41) we obtain

$$(42) \qquad k_{io} \exp(-\Delta H_i^o/RT) \prod_{j=1}^{\ell} c_j^{o\,\beta_{ij}^o} = k_{-io} \exp(\Delta H_i^o/RT) \prod_{j=\ell+1}^{n} c_j^{o\,\gamma_{ij}^o}$$

where the superscript o indicates values at saturation conditions

Thus,

$$(43) \quad \frac{k_{io}}{k_{-io}} = \prod_{j=\ell+1}^{n} c_j^{o \gamma_{ij}^o} / \prod_{j=1}^{\ell} c_j^{o \beta_{ij}^o}$$

$$i=1,\ldots,\rho$$

The r.h.s. is a constant that depends only on the values at equilibrium (chemical saturation), thus (43) can be written as

$$(44) \quad k_{-io} = \xi_i^o \, k_{io}$$

where

$$(45) \quad \xi_i^o = \prod_{j=1}^{\ell} c_j^{o \beta_{ij}^o} / \prod_{j=\ell+1}^{n} c_j^{o \gamma_{ij}^o}$$

$$i=1,\ldots\rho$$

Now, we proceed to obtain an expression for the enthalpy difference ΔH_i of reaction i. By the second law of thermodynamics the enthalpy is related to the Gibbs free energy ΔG_i via the expression

$$(46) \quad \Delta G_i = \Delta H_i - T\Delta s_i \qquad i=1,\ldots\rho$$

where Δs_i is the entropy production increment in the ith reaction and is locally given by expression (8). For variations near the chemical equilibrium point, (superscript ^{o}) the entropy production and the Gibbs free energy productions are functions only of the electrochemical potentials. Thus

$$(47) \qquad \Delta H_i = -[\sum_{j=1}^{\ell} \beta_{ij} \nabla \mu_j^o + \sum_{j=\ell+1}^{n} \gamma_{ij} \nabla \mu_j^o] + \delta_i \Delta\phi$$

$$i = 1,\ldots,p$$

This approximation is justified by the fact that the electrical potential ϕ varies much faster than the chemical potentials μ_j with systems at iso thermal conditions. The coefficient δ_i represents the drop in potential due to the ith chemical reaction.

Using (44), (47) in (41) we obtain

$$(48) \qquad s_i = k_{io}\eta_{io} \exp(-\delta_i \nabla\phi/RT) \qquad i = i,\ldots$$

where

$$\eta_{io} = \exp \{ \sum_{j=1}^{\ell} \beta_{ij} \nabla\mu_j^o + \sum_{j=\ell+1}^{n} \gamma_{ij} \nabla\mu_j^o \} \qquad i = 1,\ldots p$$

and

$$(49) \qquad s_{-i} = \xi_i^o k_{io}\eta_{io} \exp(-\delta_i \nabla\phi/RT)$$

We remark that for non-organic reactions and weak concentrations $\xi^o_i \ll 1$ (of the order of 10^{-4}).

Now, from (48) and (49) in (38),

$$(50) \qquad \sigma_i = k_{io} \eta_{io} \exp(-\delta_i \Delta\phi/RT) \; [\; \prod_{j=1}^{\ell} c_i^{\beta_{ij}} - \xi^o_i \prod_{j=\ell+1}^{n} c_i^{\gamma_{ij}} \;]$$

Finally, using (50) in (37) we obtain an expression for R_i. Thus, since the volume of reaction V remains approximately constant, (37) becomes

$$(51) \qquad R_j = \sum_{i=1}^{P} \{\alpha_{ij} k_{io} \eta_{io} \exp(-\delta_i \Delta\phi/RT) \; [\; \prod_{k=1}^{\ell} c_i^{\beta_{ik}} - \xi^o_i \prod_{k=\ell+1}^{n} c_i^{\gamma_{ik}} \;] \}$$

which gives the driving terms for equations (31). We finish this section with a formulation of initial conditions for the system of equations (31), (32) and (33).

At $t=0$ the initial concentrations are;

$$(52) \qquad c_k(0,x) = c_{k_o} \qquad\qquad k = 1,\ldots\ell$$

c_{k_o} constant, for the bulk solution species, and

$$(53) \qquad c_k(0,x) = \begin{cases} c_{k_o} & 0 \le x \le \delta, \quad L-\delta \le x \le L \\ \\ 0 & \text{otherwise} \end{cases}$$

for the reacting species, where L is the length of the system shown in figure 1.1 and δ is the reactive layer thickness, whose characteristics will be discussed later in this report.

The Boundary conditions are given by

$$(54) \qquad \phi(t,\mathscr{l}) - \phi(t,0) = \mathcal{V}(t)$$

where $\mathcal{V}(t)$ is the applied voltage to the system. Finally

$$(55) \qquad J(t) - \sum_{i=1}^{n} J_i(t,0) = 0 \qquad J(t) - \sum_{i=1}^{n} J_i(t,L) = 0$$

III. <u>Development of a Computer Algorithm for the Model of the System</u>

The algorithm, to be discussed in this section is based on the following fundamental assumption which has a strong experimental basis:

"The width, δ, of the reaction layers near the electrodes, satisfies

$$(56) \qquad \delta \ll L$$

where L is the distance between electrodes" (Newman).

The Algorithm is an adaptation of a similar one derived in (1) for active transport processes across membranes (Kohn).

The assumption given above, permits the decomposition of the system modelled by equations (31), (32), (33), (34), (35), (36) with I.C. (52) and BC (54) and (55); into three subsystems described by the following two sets of equations.

Subsystem I: Bulk Solution

$$\delta \leq x \leq L-\delta$$

Dynamics

$$\frac{\partial c_i}{\partial t} = - D_i \ RT \ \frac{\partial^2 c_i}{\partial x^2} - \nu_i F \ [\frac{\partial c_i}{\partial x} \frac{\partial \phi}{\partial x} + c_i \frac{\partial^2 \phi}{\partial x^2}]$$

$$+ F w_i \sum_{k=1}^{n} \nu_k \ [\frac{\partial c_k}{\partial x} \frac{\partial \phi}{\partial x} + c_k \frac{\partial^2 \phi}{\partial x^2}]$$

$$- \approx 0 \qquad D_i < 0$$

$$\varepsilon \frac{\partial^2 \phi}{\partial x^2} = - F \sum_{j=1}^{n} \nu_j c_j$$

$$J(t) - \sum_{i=1}^{n} J_i(x,t) + \varepsilon \frac{\partial^2 \phi}{\partial t \partial x} = 0$$

$$J_i(x,t) = \frac{\nu_i M_i J(t)}{\sum\limits_{k=1}^{n} J_k M_k} \qquad i = 1,\dots n$$

(57)

Boundary Conditions

$$\phi(t,\delta) = \psi(t,\delta) \qquad \text{(a)}$$

$$\phi(t, L-\delta) = \psi(t, L-\delta) \qquad \text{(b)}$$

where ψ is the potential distribution in the chemical layers around the electrodes

$$J(t) - \sum_{i=1}^{n} J_i(t,\delta) = \sum_{i=1}^{n} \hat{J}_i(t,\delta)$$

where $\hat{J}_i(t,\delta)$ are the current density distributions in the chemical layers

$$J(t) - \sum_{i=1}^{n} J_i(t, L-\delta) = \sum_{i=1}^{n} \hat{J}_i(t, L-\delta)$$

Subsystem II Reaction Layer

$$0 \leq x \leq \delta, \quad L-\delta < x \leq L$$

$$\frac{\partial c_i}{\partial t} = - D_i RT \frac{\partial^2 c_i}{\partial x^2} - \nu_i F \left[\frac{\partial c_i \partial \psi}{\partial x \partial x} + c_i \frac{\partial^2 \psi}{\partial x^2} \right]$$

$$+ F w_i \sum_{\substack{k \\ i \neq k}}^{n} \nu_k \left[\frac{\partial c_k}{\partial x} \frac{\partial \psi}{\partial x} + c_k \frac{\partial^2 \psi}{\partial x^2} \right]$$

$$+ \sum_{j=1}^{P} \{ \alpha_{ji} k_{jo} \eta_{jo} \exp(-\delta_j \frac{\partial \psi}{\partial x} / RT)$$

$$\left[\prod_{a=1}^{\ell} c_j^{\beta_{ja}} - \xi^o_j \prod_{a=\ell+1}^{n} c_j^{\gamma_{ja}} \right] \}$$

$$i = 1, \ldots n$$

$$\varepsilon \frac{\partial^2 \phi}{\partial x^2} = F \sum_{j=1}^{n} \nu_j c_j$$

$$J(t) - \hat{J}_i(x,t) + \varepsilon \frac{\partial^2 \psi}{\partial t \partial x} = 0, \quad \hat{J}_i(x,t) = \frac{\nu_i m_i}{\sum_{k=1}^{n} \nu_k m_k} J(t)$$

(58)

Boundary Conditions
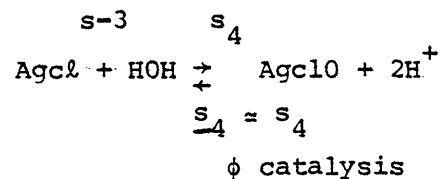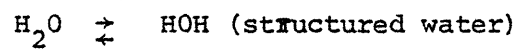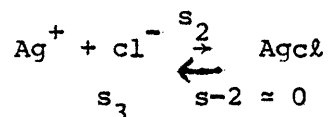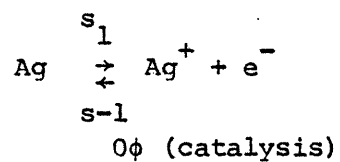
$\psi(t,0) = V(t)$ (a)

$\psi(t,\delta) = \phi(t,\delta)$ (b)

$\psi(t,L) = 0$ (c)

$\psi(t, L-\delta) = \phi(t, L-\delta)$ (d)

$\sum \hat{J}_i(0,t) - J(t) = 0 \qquad \sum \hat{J}_i(\ell,t) - J(t) = 0$ (e)

Boundary Reactions

$$\text{Ag} \underset{s\text{-}1}{\overset{s_1}{\rightleftarrows}} \text{Ag}^+ + e^-$$

$$0\phi \text{ (catalysis)}$$

$$\text{Ag}^+ + \text{cl}^- \underset{s\text{-}2 \simeq 0}{\overset{s_2}{\rightleftarrows}} \text{Agc}\ell$$

$$\text{H}_2\text{O} \underset{s\text{-}3}{\overset{s_3}{\rightleftarrows}} \text{HOH (structured water)}$$

$$\text{Agc}\ell + \text{HOH} \underset{\underline{s}_4 \simeq s_4}{\overset{s_4}{\rightleftarrows}} \text{Agc}\ell\text{O} + 2\text{H}^+$$

$$\phi \text{ catalysis}$$

Ion Species Used For Initial Simulation

Ag^+

$\text{C}\ell^-$

H_2O

HOH

H^+

$\text{AgC}\ell\text{O}$

The I.C.'s for both subsystems are given by (52) and (53).

The main idea in the algorithm, is to match the BC's (57)(a), (b) of subsystem I with the BC's (58)(b), (d) of subsystem II. Before discussing how this is carried out, let us describe the discretization scheme utilized in the computer implementation.

(59)

For first order derivatives in time;

$$\left(\frac{\partial c_j}{\partial t}\right)_{i,k} \sim \frac{1}{\Delta t}(c_j(k+1, i) - c_j(k,i))$$

For first order derivatives in space

$$\left(\frac{\partial c_j}{\partial x}\right)_{i,k} \sim \frac{1}{2\Delta x}(c_j(k, i+1) - c_j(k, i-1))$$

For second order derivatives in space

$$\left(\frac{\partial^2 c_j}{\partial x^2}\right)_{i,k} \sim \frac{1}{(\Delta x)^2}(c_j(k, i+1) - 2c_j(k,i) + c_j(k, i-1))$$

For mixed derivatives

$$\frac{\partial^2 \phi}{\partial x \partial t} \quad \frac{1}{2\Delta x \Delta t}(\phi(k+1, i+1) - \phi(k+1, i-1) - \phi(k, i+1) + \phi(k, i-1))$$

In addition for stability of the algorithm, $\left|\frac{\Delta t}{\Delta x}\right| \leq 1$ typically, $\Delta t = 1/4 \ \Delta x$. Lions et al.

Scheme (59) applied to (57) and (58) gives two sets of difference equations that can be implemented in a computer. In the actual implementation of the algorithm to be described in the next section, a digital integration method with a sliding (spatial) window was devised, due to the high dimensionality of the problem.

Now we can describe the algorithm.

step (0)   set $t = 0$ (t = time)

step (1)   set $\ell = 0$

step (2)   let $\delta = \delta^{(\ell)}$

comment: δ^0 is assumed initially typically, $\delta^0 = 1/100 \ L$.

step (3)   set $\ell_1 = 0$

step (4)   set $\phi^{(\ell_1)}(t, \delta^{(\ell)}) = \psi^{(\ell_1)}(t, \delta^{(\ell)})$

comment: ψ^0 is assumed initially typically $\psi^{(0)}(t, \delta^{(\ell)}) = .4V(t)$

step (5)   Integrate subsystem II in space between $x = \delta$ and $x = L-\delta$ i.e., obtain $\phi^{(\ell_1)}(t, \ L-\delta)$

step (6)   Integrate subsystem II in space i.e., obtain $\psi^{(\ell_1)}(t, \ 0)$, $\psi^{(\ell_1)}(t, \ L)$

step (7)   If $\psi^{(\ell_1)}(t, \ 0), = V(t)$, $\psi^{(\ell_1)}(t, \ L) = 0$ go to (10) otherwise go to (8)

step (8)   set $\psi^{(\ell_1+1)}(t, \delta^{(\ell)}) \leftarrow \psi^{(\ell_i)}(t, \delta^{(\ell)} + H\psi_{1\ell_1} \ |\psi^{(\ell_1)}(t, 0) - V(t)|$ $+ \ H\psi_{2\ell_1} \ |\psi^{(\ell_1)}(t, \ L)|$

comment: $H\psi_{2\ell 1}$ $H\psi_{2_{\ell 1}}$ are suitably chosen gains

step (9) $\ell_1 \leftarrow \ell_1 + 1$ Go to 4

step (10) If $J(t) - \sum_i \hat{J}_i(t,0) = 0$ and $J(t) - \sum_i \hat{J}_i(t,L) = 0$ Go to (14)

otherwise go to (11)

step (11) set $\delta^{(\ell+1)} \leftarrow \delta^{(\ell)} + M_{\delta_1 \ell}\left| J(t) - \sum J_i(t,0) \right| + M\delta_2 \ell \left| J(t) - \sum J_i(t,L) \right|$

comment: $M\delta_1 \ell$, $M\delta_2 \ell$ are suitably chosen gains

step (12) set $\psi^{(o)}(t,\delta^{(\ell)}) \leftarrow \psi^{(\ell_1)}(t,\delta^{(\ell)})$

step (13) set $\ell \leftarrow \ell+1$ Go to setp (3)

step (14) set $t \leftarrow t+\Delta t$ Go to (1)

The algorithm works as follows: it considers an initially given re-
action layer width δ^o, and an initially given B.C. $\psi^{(o)}(t, \delta)$. It integrates
both subsystems and iterates until the potential B.C. of the two subsystems
match. Once this is done, it checks the current B.C's of the subsystem II,
if they match with the given value $J(t)$ it repeats the whole process for a
new value of time $t+\Delta t$; if they do not match, it changes the value of δ and
starts the potential iteration again.

REFERENCES

Geddes, L.A., _Electrodes and the Measurement of Bioelectrics Events_, Wiley-Interscience, N.Y., 1972.

> An introduction to the area of electrodes and bioelectric measurement - discusses the impedance of Ag-AgCl electrodes and the chloriding process itself - contains a chapter on surface electrodes in general (with an historical account) - describes an experiment for investigating the impedance of the elctrode-electrolyte interface (similar to our initial experiment).

Parsons, R., "The Structure of the Electrical Double Layer and Its Influence on the Rates of Electrode Reactions," Adv. in Electrochem. and Electrochem. Engr., Volume 1, pp. 1-60 (1961).

> Discusses the ionic double layer for the Mercury electrode - the effect of the double layer on the rates of electrode reactions is described by an electrostatic model.

Newman, J., "Transport Processes in Electrolytic Solutions," _Adv. in Electrochem. and Electrochem. Engr._, Volume 5, pp. 88-135 (1966).

> Contains macroscopic laws describing migration and diffusion in electrolytic solutions - describes transport in dilute and concentrated electrolytes and boundary conditions - includes the Nernst-Einstein Relation, conservation relations, and the eq. of convective diffusion and also Ousager's modification for concentrated solutions.

Barlow, C.A. Jr. and MacDonald, J.R., "Theory of Discreteness of Charge Effects in the Electrolyte Compact Double Layer," _Adv. in Electrochem. and Electrochem. Engr._, Volume 6, pp. 1-195 (1967).

> Discusses some theories about effects of the finite size of the changed particles in the double layer.

Schiffrin, D.J., "Ionic Double Layers and Absorption," _Electrochemistry_, Volume 2, pp. 169-202 (1972).

> Contains a review of the literature of 1970 on double layers and absorption - most of the results are for Mercury and Platinum - "relatively limited activity in the study of theoretical aspects of absorption and inner layer theory."

Electrochemistry, Volume 3, chapter 3 (1973).

> Analyzes the phase transition (solid formation) problem at the double layer.

Watanabe, "Ag-AgCl Double Layer and Structural Water," _Electrochemistry_, Volume 4 (1974).

> Gives an experimental account of energy losses due to the formation of water dipoles in the neighborhood of the electrodes - also covers the catalytic effect of these dipoles on the formation of AgCl.

Lightfoot, J., <u>Transport Phenomena,</u> John Wiley, N.Y., 1958.

A theoretical development of energy and momentum equations in electrolytic systems in terms of the Gibbs-Dunhem theory (chapter 6).

References for the initial handout on the balance equations:

[1] Priggogini, A., <u>Principles of Nonequilibrium Thermodynamics,</u> Springer-Berlag, 1967.

[2] Katchalsky, A. and Curran, R., <u>Biology of Irreversible Thermodynamics in Membrane Systems,</u> Harvard Press, 1970.

[3] Gyamarty, L., <u>Irreversible Thermodynamics and Generalized Field Theory,</u> Chapter 5, John Wiley, N.Y., 1972.

[4] Kadem, B. and Katchalsky, A., <u>Equilibrium Theory in Nonreversible Systems,</u> Harvard Press, 1968.

[5] Magur, H. and DeGroot, <u>On Onsager Relationships,</u> Academic Press, 1962.

Secondary References:

Electrochemistry Specialist Periodic Reports, Volume 1.

H.C. Gaur and R.G. Sethi, Electrochem Act a 1968 13, 1737, Heats and Free Energies of Solution for AgCl.

F. Anson, Ann. Rev. Phys. Chem. 1968 1983

O. Dracka, Coll. Czech. Chem. Comm. 1969 34 26 27, When to Neglect Influence of Double-Layer Charging.

P. Delahay, J. Phys. and Chem. 1966, 70, 2373. Double layer and charge transfer processed not separable "a priori."

A. D. Graves, G.J. Hills, D. Inman, Advances in Electrochemistry and electrochemical Engineering, ed. P. Delayhay, 1966 4 117. Double-layer charging may be separated instrumentally from change transfer and diffusion processes, e.g., by making measurememnts at sufficiently short times.

C.G.J. Baker, E.R. Buckle, Trans. Faraday Soc. 1968 64 469, Space charge polarization model.

E.V. Panov, A.V. Gorodyskii, Ukrain. Khim. Zhur. 1968 34 305, Instrumental technique ofr recording impedance automatically.

J.N. Slayters in Electroanalytical Chemistry, Volume 4, ed. by A.J. Bard, Marcel Dekker, New York.

P.D Power (British) Society for Electorchemistry, Review of aqueous literature.

Ives, D. and Janz, G., Reference Electrodes, Acad. Press, 1961

Thirsk, H. R. and Harrison, J., A Guide to the Study of Electrode Kinetics, Acad. Press, 1972

Delahay, P., Double Layer and Electrode Kinetics, Interscience Pub., New York, 1965

Yeager, E. and Salkind, A. J., Techniques of Electrochemistry, Vol1 Wiley-Interscience, N. Y. 1972

Bockris, J. O'M. and Reddy, A.K.N., Modern Electrochemistry, Vol. 2, Plenum Press, 1967

Vetter, K. J., Electrochemical Kinetics, Academic Press, New York, 1967

Lyklema, J. and Overbeek, J. Th. G., "Electrochemistry of Silver Iodide", J. Colloid Science, Vol. 16, p. 595-608 (1961)

Lyklema, J., "Electrical Double Layer on Silver Iodide", Dicc. Faraday Soc., Vol. 42, p. 81-90 (1966)

Beruke, Y. G. and Debruyn, P. L., "Adsorption at the Rutile-Solution Interface", J. Colloid and Interface Science, Vol. 28, p. 92-105 (1968)

Janz, G. J. and Ives, D.J.G., "Silver, Silver Chloride Electrodes", Annals of N.Y. Acad. of Sciences, Vol. 148, Art. 1, pp. 210-221

Eyring, E. M., Modern Chemical Kinetics, New York, Reinhold Publishing Co. (1963)

Ferris, C. D. and Stewart, L. R., "Electrode-Produced Distortion in Electro-physiological Recording Systems", IEEE Trans. Biomed. Eng., Vol. 21, No. 4 (1974)